
# Ideal Polymers: Equilibrium Properties from Non-equilibrium Processes

Thesis submitted as part of the requirements for the degree of
Master of Science (M.Sc.) in Physics at Tel Aviv University
School of Physics and Astronomy

by

**Raz Halifa-Levi**

The research work for this thesis was carried out
under the supervision of **Prof. Yacov Kantor**

July 2016

# Acknowledgments

I would like to thank my supervisor, Professor Yacov Kantor, whose guidance, support and endless patience enabled me to study and understand the field of polymers, and complete this thesis. I also wish to thank Mr. Yosi Hammer for his insightful advice and guidance.

# Abstract

Stretching experiments in bio-molecules are increasingly used to extract the free energy profiles of such molecules. In order to measure the free energy landscape, these experiments should be sufficiently slow to keep the system in equilibrium. In practice, quite frequently these measurements are out of equilibrium [1]. Nevertheless, if the deviation from equilibrium is not too strong, the free energy profiles can be extracted from a repeated non-equilibrium experiment, by using the Jarzynski equality [2, 3]. We can learn about the behavior of such systems by examining the simple model of an ideal polymer.

We consider several cases of an ideal polymer being dragged by an external force during a finite time. The work $W$ in such a process depends on the initial state of the polymer. By repeating this process multiple times (for different initial states), we get the probability distribution $P(W)$ of the work. The free energy difference between the initial state and the final (equilibrated) state $\Delta F$, can be extracted from the calculated $P(W)$, provided the deviation from equilibrium is not too strong. If we know $P(W)$ analytically, we can always find $\Delta F$. We consider both Newtonian dynamics and overdamped Langevin equations, for a polymer that is moving either in free space, or is initially located near a repulsive wall. In all cases one end of a polymer is dragged with a constant velocity $v$.

We calculate $P(W)$ (either analytically or numerically), and demonstrate that there is a critical velocity $v_c$, such that for $v \ll v_c$ the $\Delta F$ can be easily reconstructed, while for $v > v_c$ such reconstruction is, practically, impossible. We determine the dependence of $v_c$ on the number of monomers $N$.

# Contents

# Chapter 1
# Introduction

## 1.1 Simple polymer models

A polymer is a long molecule consisting of repeating elementary units called monomers. Monomers are connected to each other by covalent bonds. At room temperature, the bond energy $\gg k_{\mathrm{B}}T$, where $k_{\mathrm{B}}$ is the Boltzmann constant and $T$ is the temperature. The number of monomers $N$ defines the degree of the polymer. Polymers in which all the monomers are identical are called *homopolymers*, and polymers which contain several types of monomers are known as *heteropolymers*.

Polymer systems have been subject to extensive study for many decades [4–6]. The interest in such macro-molecules arises mainly from their natural occurrence in biological systems, e.g., DNA and proteins. Artificial polymers are very common in everyday life and are of great commercial and industrial value. Flexible polymers are characterized by an enormous number of spatial configurations. Therefore, the shape of the polymers can only be usefully described statistically. Since the mid - 20th century, much effort has gone into constructing physical models describing the statistical behavior of polymers. The simplest model to describe a linear polymer chain is the *ideal chain model*. This model disregards interactions between monomers that are not nearest-neighbors along the chain, even if they occupy the same place in space. This situation is obviously impossible for real polymers, but there are several types of polymeric systems that resemble the ideal chain model. Such a system for example, is a polymeric dilute solution in a solvent at a special temperature, called the $\Theta$-temperature. Another reason for using the ideal chain model is simplification of the mathematical treatment.

Consider a linear chain with $N+1$ monomers (numbered 0 to $N$). We denote by $\mathbf{R}_i$ the vector from some origin to the $i$th monomer, and $\mathbf{r}_i \equiv \mathbf{R}_i - \mathbf{R}_{i-1}$ the bond vector that goes from the $(i-1)$th monomer to the $i$th monomer. The simplest means of describing the size of the polymer is the *end-to-end vector* $\mathbf{R}_{\mathrm{ee}}$, which is the vector connecting the zeroth monomer to the last monomer

$$\mathbf{R}_{\mathrm{ee}} = \mathbf{R}_N - \mathbf{R}_0 = \sum_{i=1}^{N} \mathbf{r}_i. \tag{1.1}$$

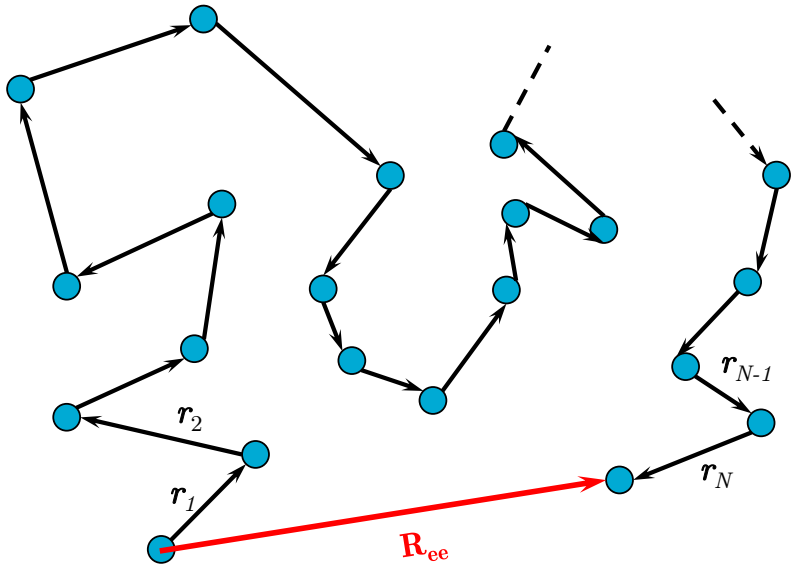


**Figure 1.1:** An ideal polymer of $N+1$ monomers presented as $N$ random steps.

Another measure for the size of the polymer called *radius of gyration* [5] $R_g$ defined via

$$R_g^2 = \frac{1}{N+1}\sum_{i=0}^{N}\left\langle(\mathbf{R}_i - \mathbf{R}_{\rm cm})^2\right\rangle, \tag{1.2}$$

where $\langle\cdots\rangle$ denotes average over all the spatial configurations of the polymer, and $\mathbf{R}_{\rm cm}$ is the position vector of the polymer's center of mass

$$\mathbf{R}_{\rm cm} = \frac{1}{N+1}\sum_{i=0}^{N}\mathbf{R}_i. \tag{1.3}$$

### 1.1.1 Freely jointed chain

A simple realization of a polymer could be that of equally separated monomers, with constant $|\mathbf{r}_i| = a$. In free space, the system is rotationally invariant, and therefore,the mean end-to-end distance $\langle\mathbf{R}_{\rm ee}\rangle = 0$. The size of the chain is therefore characterized

by the root-mean-square (r.m.s) end-to-end distance defined via

$$R^2 = \left\langle \mathbf{R}_{\rm ee}^2 \right\rangle \tag{1.4}$$

$$= \sum_{i,j=1}^{N} \left\langle \mathbf{r}_i \cdot \mathbf{r}_j \right\rangle . \tag{1.5}$$

The average $\langle \mathbf{r}_i \cdot \mathbf{r}_j \rangle = a^2 \delta_{ij}$ because there is no correlation between the directions of different bond vectors. Thus

$$R = a\sqrt{N}. \tag{1.6}$$

Generally, $R$ can be related to the number of monomers $N$ as

$$R = aN^{\nu}, \tag{1.7}$$

where the exponent $\nu = \frac{1}{2}$ for ideal polymers, but can be larger for polymers in good solvents.

### 1.1.2 Random walks and ideal polymers

Consider a particle making a random walk [7, 8] with a constant step size $|\mathbf{r}_i| = a$. The trajectory of this random walk is one conformation of a freely jointed chain. According to the central limit theorem, the distribution of the sum $\mathbf{R}_{\rm ee} = \sum_{i=1}^{N} \mathbf{r}_i$ of $N \gg 1$ random variables that have finite variance will be Gaussian. Thus, we get the distribution of the end-to-end vector

$$P_N(\mathbf{R}_{\rm ee}) = \left( \frac{d}{2\pi N a^2} \right)^{\frac{d}{2}} e^{-\frac{d\mathbf{R}_{\rm ee}^2}{2Na^2}}, \tag{1.8}$$

where $d$ is the space dimension.

The entropy of the chain is related to the number of available configurations $\mathcal{N}_N$ as

$$S(\mathbf{R}_{\rm ee}) = k_{\rm B} \ln \mathcal{N}_N = S(0) - \frac{d}{2} k_{\rm B} \frac{\mathbf{R}_{\rm ee}^2}{Na^2}. \tag{1.9}$$

The free energy $F$ of the chain can be obtained from the entropy as $F = U - TS$, where $U$ is the internal energy. Taking into account the fact that $U$ in ideal polymers does not depend on $\mathbf{R}_{\rm ee}$ we get

$$F_N(\mathbf{R}_{\rm ee}) = \frac{1}{2} \frac{d k_{\rm B} T}{Na^2} \mathbf{R}_{\rm ee}^2 + F_N(0). \tag{1.10}$$

This can be interpreted as an energy of a long spring with an effective spring constant $k_{\text{eff}} = \frac{dk_{\text{B}}T}{Na^2}$. This is an *entropic spring*, since the source of the free energy is the large number of chain conformations.

### 1.1.3 Gaussian chain

The same distribution as (1.8) can be obtained by initially taking a bond length that has a Gaussian distribution [6, 9]

$$P(\mathbf{r}_i) = \left(\frac{d}{2\pi a^2}\right)^{\frac{d}{2}} e^{-\frac{d\mathbf{r}_i^2}{2a^2}}. \tag{1.11}$$

In other words, in $d = 3$ case we can replace the bonds by springs with a spring constant $k = \frac{3k_{\text{B}}T}{a^2}$.

Consider a linear chain of $N + 1$ monomers connected by such springs. The unstretched lengths of the springs is zero. All the monomers have the same mass $m$ and all the springs have the same spring constant $k$. The potential energy of the system is

$$V = \frac{1}{2}k\sum_{i=1}^{N}(\mathbf{R}_i - \mathbf{R}_{i-1})^2 = \frac{1}{2}k\sum_{i=1}^{N}\mathbf{r}_i^2. \tag{1.12}$$

Any sub-chain of a Gaussian chain is also a Gaussian chain no matter what is the size of the sub-chain.

Figure 1.2 depicts an illustration of a Gaussian chain. Notice, that the fact that the unstretched length of the springs is zero, lead to decomposition of the potential to $d$ independent directions, which allow us to deal with only one direction ($x$ coordinate). For that reason, we consider only the 1D Gaussian system, and the other directions will not influence our calculations.

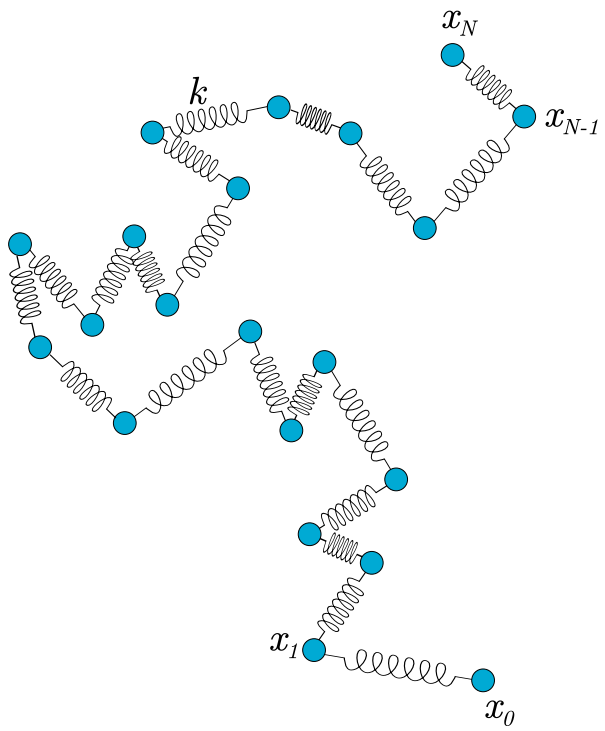


**Figure 1.2:** Illustration of a Gaussian chain consisting of $N + 1$ monomers and $N$ springs with spring constant $k$. We consider only 1D Gaussian chains in this thesis. The second dimension is for illustration only.

# Chapter 2

# Review of Relevant Results

## 2.1 Ideal polymers near a repulsive wall

Equilibrium interaction between polymers and repulsive surfaces have been a subject of intensive study for the last several decades. Current experimental methods allow a detailed study of biological macro-molecules [10]. In particular, the atomic force microscopy [11] (AFM) is an important tool in measuring force-displacement curves of bio-molecules, and reconstructing their free energy profile [12].

Figure 2.1 depicts an ideal polymer that is held in equilibrium at distance $x$ of the end-monomer from a plane, while its other end is free. When $x$ is much larger then the microscopic distance $a$, and samller than the root-mean-square end-to-end distance $R$ of the polymer, then it becomes the only relevant quantity that has dimensions of distance. From purely dimensional considerations the equilibrium force that the wall applies on the polymer is given by [13–15]

$$f_{\text{wall}} = \mathcal{A}\frac{k_{\text{B}}T}{x}, \tag{2.1}$$

where $\mathcal{A}$ is a dimensionless prefactor. Expression (2.1) is more general, and valid also for a polymer in a vicinity of *scale-free* surface, i.e., surface that does not change its geometry under compressing or stretching transformation $\mathbf{r} \to \lambda\mathbf{r}$. It has been shown [13] that the value of the prefactor $\mathcal{A}$ depends only on the critical exponents characterizing the scale-free surface. The free energy difference $\Delta F$ between the initial state (where the polymer is near the wall $x \approx a$), and the final state (where the polymer is far away from the wall $x \approx R$) can be calculated from by integrating 2.1:

$$\Delta F = -\int_{a}^{R=aN^{\nu}} \mathcal{A}\frac{k_{\text{B}}T}{x}dx = -\mathcal{A}k_{\text{B}}T\nu\ln N. \tag{2.2}$$

Notice, that since the limits of the integration are approximated, this expression to the free energy difference is valid up to a constant term. When a very long flexible polymer is located near a repulsive wall, the number of its available configurations is reduced relative to being in free space. In general, the number of configurations

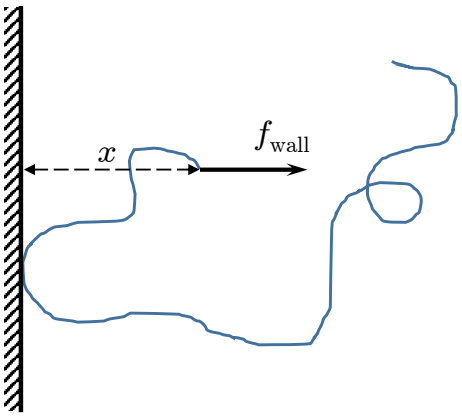


**Figure 2.1:** A polymer is held by its end near a repulsive wall. A force $f_{\text{wall}}$ exerted to its end by the wall. Positive direction of the force is defined away from the wall. If we want to keep the polymer at equilibrium we must apply a force $-f_{\text{wall}}$ on its end to counteract the repulsion of the wall.

is given by

$$\mathcal{N}_N \propto z^N N^{\gamma-1}, \tag{2.3}$$

where $z$ is the effective coordination number and $\gamma$ is a universal exponent. For ideal polymers near a rigid wall, it can be shown by the method of images [16], that $\gamma_w = \frac{1}{2}$ ("$w$" denotes wall), while for ideal polymers in free space $\gamma_f = 1$ ("$f$" denotes free space). Thus, $\Delta F$ can be calculated from the entropy change $\Delta S$ between the initial and final states:

$$\begin{aligned} \Delta F &= -T\Delta S \\ &= -T\left[k_{\text{B}} \ln\left(N^{\gamma_f - 1}\right) - k_{\text{B}} \ln\left(N^{\gamma_w - 1}\right)\right] \\ &= -\left(\gamma_f - \gamma_w\right) k_{\text{B}} T \ln N. \end{aligned} \tag{2.4}$$

Since (2.3) is valid up to a proportionality constant, the expression (2.4) for the free energy is valid up to a constant term. Equating (2.2) with (2.4) yields the prefactor

$$\mathcal{A} = \frac{\gamma_f - \gamma_w}{\nu}. \tag{2.5}$$

Since the exponent $\nu = \frac{1}{2}$, we simply get that $\mathcal{A} = 1$.

## 2.2 Non-equilibrium processes

Consider an arbitrary system which is initially in equilibrium with a thermal bath, i.e., the initial state is chosen from a canonical ensemble. An external work $W$ can be performed to bring the system from the initial state to another state. Then we let the system equilibrate to a final state by keeping it in contact with the same thermal bath it contacted in the beginning. The free energy difference between the final and the initial states is denoted $\Delta F$. It is known from elementary thermodynamics that when a system is driven from the initial to the final state by an isothermal reversible process, then the work $W = \Delta F$. If, in contrast, the process connecting initial and final states is irreversible, $W$ might depend on the initial state and details of the process, and therefore vary upon repetition of the process with $\langle W \rangle \geq \Delta F$, where $\langle \cdots \rangle$ denotes a thermal average over initial states and changes during the process.

A remarkable relation derived by Jarzynski [2] relates the distribution $P(W)$ of the non-equilibrium work $W$ to the equilibrium free energy difference $\Delta F$ by

$$\left\langle e^{-\beta W} \right\rangle = \int_{-\infty}^{\infty} e^{-\beta W} P(W) \mathrm{d}W = e^{-\beta \Delta F}, \tag{2.6}$$

where $\beta = 1/k_{\mathrm{B}}T$. Thus, $\Delta F$ can be expressed in terms of $P(W)$ as

$$\Delta F = -\frac{1}{\beta} \ln \left( \int_{-\infty}^{\infty} e^{-\beta W} P(W) \mathrm{d}W \right). \tag{2.7}$$

Reconstruction of $\Delta F$ can be understood as measurement of the area $A$ under function $f(W) = e^{-\beta W} P(W)$. In order to reconstruct $A$ correctly, we need to sample values of $W$ around the peak of $f(W)$. Usually, $f(W)$ is shifted from $P(W)$ towards the lower values of $W$ so that the peak of $f(W)$ is located on the tail of $P(W)$, as shown in Figure 2.2. In other words, the values of work which significantly contribute to $\Delta F$ arise only rarely. An accurate estimate of $\Delta F$ hence requires proper sampling of those rare work values. In order to reconstruct $\Delta F$ correctly we must have a substantial overlap between $P(W)$ and $f(W)$.

An interesting question could be asked: What is the probability to get values of work that smaller than $\Delta F$ by $\xi$? In other words, what is the probability to violate

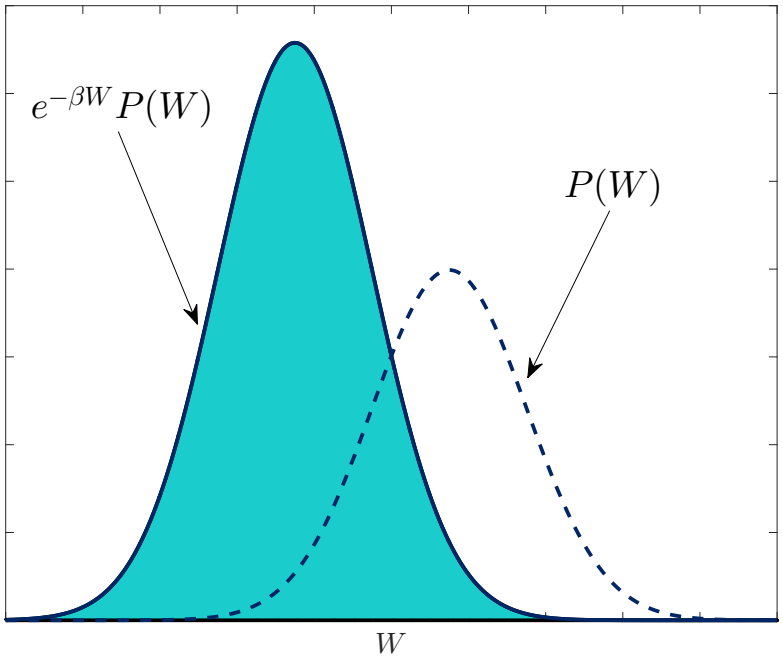


**Figure 2.2:** The distribution of work $P(W)$ and the shifted function $f(W) = e^{-\beta W}P(W)$. We can see that when the shift between these function is large, there is little overlap between them. Thus, if the functions are too shifted from each other, the probability to reconstruct the area under $f(W)$ is zero.

the second law of the thermodynamics? The answer [17] follows from (2.6):

$$\begin{aligned}
\text{Prob}(W < \Delta F - \xi) &= \int_{-\infty}^{\Delta F-\xi} P(W)dW && (2.8)\\
&\leq \int_{-\infty}^{\Delta F-\xi} P(W)e^{(\Delta F-\xi-W)/k_{\mathrm{B}}T}dW && (2.9)\\
&\leq e^{(\Delta F-\xi)/k_{\mathrm{B}}T}\int_{-\infty}^{\Delta F-\xi} P(W)e^{-W/k_{\mathrm{B}}T}dW && (2.10)\\
&= e^{-\xi/k_{\mathrm{B}}T}. && (2.11)
\end{aligned}$$

Thus, if $\xi$ is larger than a few $k_{\mathrm{B}}T$ we have no reasonable hope to measure work values that violate the second law of the thermodynamics. Notice, that this constraint does

not depend on the size of the system.

Generally, we can expand the logarithm of the exponential average in (2.7) in terms of cumulants [2, 18]

$$\Delta F = \mu - \frac{\beta}{2}\sigma^2 + ... \tag{2.12}$$

where $\mu = \langle W \rangle$ and $\sigma^2 = \left\langle (W - \langle W \rangle)^2 \right\rangle$. If $P(W)$ is a Gaussian centered around an average $\mu$ with width $\sigma$

$$P(W) = \frac{1}{\sqrt{2\pi}\sigma} e^{-\frac{(W-\mu)^2}{2\sigma^2}}, \tag{2.13}$$

the cumulant expansion (2.12) is truncated at the second order [2], i.e., the terms beyond $\sigma^2$ are absent, and we get a simple relation between the free energy difference and the mean and variance of the work

$$\Delta F = \mu - \frac{\beta}{2}\sigma^2. \tag{2.14}$$

It had been shown, that for slow processes in general diffusive systems the distribution of work is indeed Gaussian [19, 20]. For the case of Gaussian distributions with $\Delta F = 0$, i.e., $\mu = \frac{\beta}{2}\sigma^2$, we find that $f(W)$ is another Gaussian centered around $-\mu$. In other words, $f(W)$ is shifted to the left by $2\mu$. Therefore, in order to have a substantial overlap between $P(W)$ and $f(W)$ we demand that

$$\mu \ll \sigma. \tag{2.15}$$

Experimental tests [1, 21–29] and numerical simulations [30–34] of the classical Jarzynski equality have been successfully performed in various systems, as well as for quantum systems [35, 36].

# Chapter 3

# Dragging a Polymer in Free Space

In this chapter we consider the problem of 1D Gaussian chain being dragged with a constant velocity $v$ in free space during time $t$. The end of the chain, i.e., the monomer numbered 0, is being dragged from one place ($x_0 = 0$) to another ($x_0 = vt$), as depicted in Figure 4.1. The problem is solved analytically both for Newtonian dynamics (zero friction and no thermal noise) and overdamped Langevin dynamics, where the inertial terms are neglected. Both cases posses a natural time scales which are set either by the natural frequency of the spring in the Newtonian case, or by the friction constant in the overdamped case. We verify the Jarzynski equality, and find the critical pulling velocity for which Jarzynski equality can be practically used to reconstruct the free energy difference $\Delta F$ between two different equilibrium states of the chain (for numerically calculated $P(W)$).

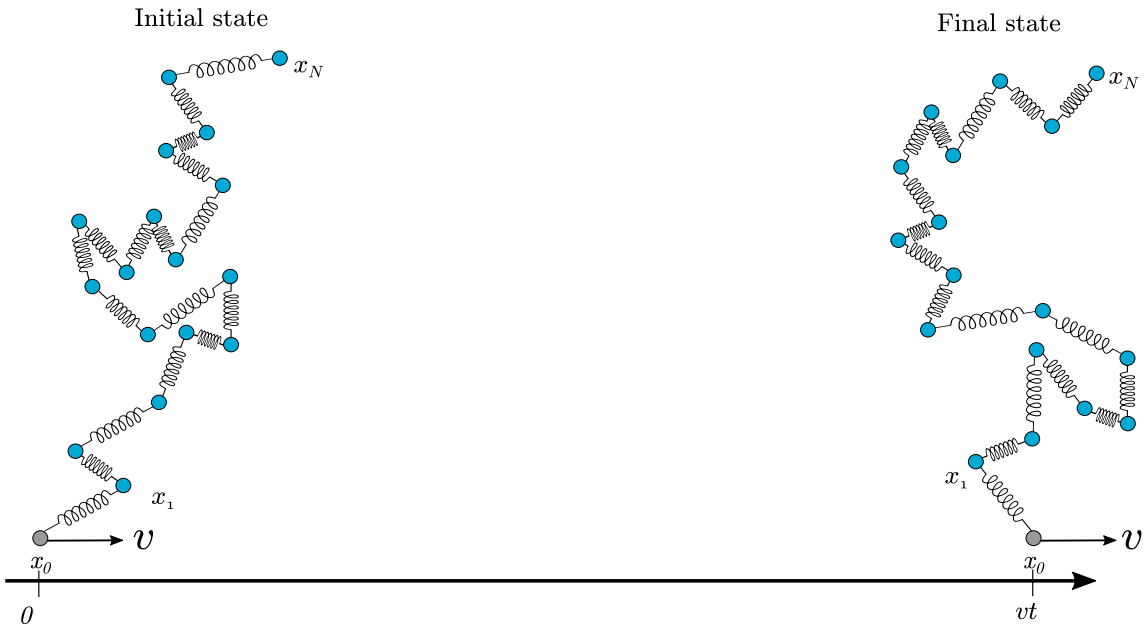


**Figure 3.1:** A Gaussian chain is being dragged by its end with a velocity $v$ along distance $vt$. We are interested in the distribution of work done on the polymer during the pulling. Notice, that we consider only 1D Gaussian chains, and the second dimension is for illustration only.

## 3.1 Newtonian dynamics

In this section we consider a harmonic oscillator or a Gaussian chain whose dynamics is governed by Newton's laws of motion. The chain is initially in equilibrium and coupled to a thermal bath with a certain temperature $T$. At time $t = 0$ we disconnect the chain from the thermal bath and start dragging its end with a constant velocity $v$ during time $t$. At the end of the process we connect the system again to a thermal bath with the same temperature and let the system relax to an equilibrium state. The free energy difference $\Delta F$ is measured between the initial equilibrium state and the final equilibrium state. We start with the case of single harmonic oscillator ($N = 1$) and generalize it for the case of a Gaussian chain ($N > 1$)

### 3.1.1 Single oscillator

Consider the motion of a particle of a mass $m$ at position $x_1$ attached by a spring with force constant $k$ to a point $x_0$, which moves with velocity $v$, i.e., at time $t$ its position is $x_0 = vt$. Such a motion is described by Newton's equation

$$m\ddot{x}_1 = -k(x_1 - vt). \tag{3.1}$$

Since the mass $m$ and the spring constant $k$ define an elementary frequency $\omega = \sqrt{k/m}$, we can simplify our equation by using dimensionless time, i.e., $\omega^{-1}t = \sqrt{k/m}t \to t$. Our calculations will be performed at temperature $T$, which can be used to define dimensionless velocity $\sqrt{m/k_{\mathrm{B}}T}v \to v$, as well as dimensionless distance $\sqrt{k/k_{\mathrm{B}}T}x \to x$. The energy will be measured in units of $k_{\mathrm{B}}T$, which corresponds to setting $k_{\mathrm{B}}T = 1$. In these dimensionless variables the momentum $p$ coincides with the velocity, the Hamiltonian (energy) of the system becomes $\frac{1}{2}p_1^2 + \frac{1}{2}(x_1 - vt)^2$, and the equation of motion becomes

$$\ddot{x}_1 = -(x_1 - vt). \tag{3.2}$$

The transformation from dimensionless to dimensional variables is detailed in Appendix A. (In the next section we will consider an overdamped motion of a particle, which will require a different choice of dimensionless time units.)

The system is initially connected to a thermal bath so that the initial values of the canonical variables, position $x_1^0$ and momentum $p_1^0$, are chosen from a canonical

ensemble with the probability

$$\rho(x_1^0, p_1^0) = \frac{1}{2\pi} \exp\left[-\frac{1}{2}\left(x_1^0\right)^2 - \frac{1}{2}\left(p_1^0\right)^2\right]. \tag{3.3}$$

At time $t = 0$ we disconnect the system from the thermal bath and start moving $x_0$ with a constant velocity $v$ ($x_0 = vt$) by applying a force $f$. Notice that the force is not determined by external constraint, but rather is such that it maintains a constant velocity $v$. After time $t$ we stop, connect the system to the thermal bath again and let it reach the equilibrium. The free energy difference $\Delta F$ between the initial state and the final state is zero, because it does not matter where $x_0$ is located in the space. The solution of the equation of motion (3.2) is

$$x_1(t) = x_1^0 \cos t + \left(p_1^0 - v\right) \sin t + vt. \tag{3.4}$$

The work done by the force $f$ is

$$\begin{aligned} W(x_1^0, p_1^0) &= -v \int_0^t (x_1 - vt')\, dt' \\ &= -v\left[x_1^0 \sin t - \left(p_1^0 - v\right)(\cos t - 1)\right]. \end{aligned} \tag{3.5}$$

Repeating this process for different initial conditions produces work distribution $P(W)$. The work $W$ is a linear function of the Gaussian variables $x_1^0$ and $p_1^0$, therefore $P(W)$ is a Gaussian characterized by its mean $\mu = \langle W \rangle$ and variance $\sigma^2 = \langle W^2 \rangle - \langle W \rangle^2$. From (3.3) we can see that $\langle x_1^0 \rangle = \langle p_1^0 \rangle = 0$ and $\left\langle \left(x_1^0\right)^2 \right\rangle = \left\langle \left(p_1^0\right)^2 \right\rangle = 1$. Therefore, the mean work is given by

$$\langle W \rangle = 2v^2 \sin^2\left(\frac{t}{2}\right), \tag{3.6}$$

and the mean squared value of work is given by

$$\left\langle W^2 \right\rangle = 4v^2 \sin^2\left(\frac{t}{2}\right). \tag{3.7}$$

Thus, we get a relation between the mean and the variance of work

$$\mu(t) = \frac{1}{2}\sigma^2(t) = 2v^2 \sin^2\left(\frac{t}{2}\right). \tag{3.8}$$

Notice, that the mean value of $W$ vanishes every complete period, i.e., when $t$ is an integer multiple of $2\pi$. Indeed, Jarzynski equality gives us $\Delta F = \mu - \frac{1}{2}\sigma^2 = 0$ for this case. We can see that the typical value of $\mu$ is $v^2$, thus requirement (2.15) yields a condition on the pulling velocity $v \ll 1$. The critical case is when $\mu \approx \sigma$, which defines the critical velocity

$$v_c \approx 1. \tag{3.9}$$

If we restore the dimensions to the velocity, this means that in order to reconstruct $\Delta F$ correctly the pulling velocity should not exceed the typical thermal velocity $v_c \approx \sqrt{k_{\mathrm{B}}T/m}$.

### 3.1.2 1D polymer

Consider a 1D Gaussian chain of $N$ identical monomers. The positions and the momenta of the monomers are $\{x_n\}_{n=1}^N$ and $\{p_n\}_{n=1}^N$. The first monomer is connected to a point $x_0$ by a harmonic spring. The polymer is being dragged by moving $x_0$ with constant velocity $v$ during time $t$, i.e., $x_0 = vt$. The equation of motion of the $n$th monomer, for $1 \leq n \leq N-1$ in the laboratory reference frame is given by

$$\ddot{x}_n = -2x_n + x_{n+1} + x_{n-1}, \tag{3.10}$$

and for $n = N$

$$\ddot{x}_N = -x_N + x_{N-1}. \tag{3.11}$$

In Appendix B, we show that working in the *moving reference frame*, where $\tilde{x}_n = x_n - vt$, the system can be decomposed into $N$ eigenmodes (called phonons in mechanics and Rouse modes [6] in polymer physics) by performing a discrete sine Fourier transform

$$x_n = A\sum_{q=1}^{N} \tilde{x}_q \sin(\alpha_q n) + vt, \tag{3.12}$$

where $\tilde{x}_q$ is the amplitude of the $q$th mode with respect to the moving reference frame and

$$A = \sqrt{\frac{2}{N+\frac{1}{2}}} \quad ; \quad \alpha_q = \frac{\pi(q-\frac{1}{2})}{N+\frac{1}{2}} \ . \tag{3.13}$$

We chose the sine transform and these values of $\alpha_q$ to satisfy the boundary conditions, where we demanded that one end of the polymer is moving with constant velocity $x_0 = vt$, and the other end is "free", i.e., the only force acting on the $N$th monomer is

the force applied by the $(N-1)$th monomer. It is convenient to present the constant velocity $v$ as

$$v = A\sum_{q=1}^{N} v_q \sin(\alpha_q n), \tag{3.14}$$

where

$$v_q = \frac{1}{2} A v \cot\left(\frac{\alpha_q}{2}\right), \tag{3.15}$$

and $q = 1, 2, .., N$. Notice that (3.14) is correct for any $1 \leq n \leq N$. This way the problem completely separates into set of $N$ independent differential equations

$$\ddot{x}_q = -\omega_q^2 (x_q - v_q t), \tag{3.16}$$

where $x_q$ is the amplitude of the $q$th mode with respect to the laboratory reference frame, and

$$\omega_q^2 = 4\sin^2\left(\frac{\alpha_q}{2}\right). \tag{3.17}$$

This can be understood as $N$ independent oscillators. Each oscillator has its own frequency $\omega_q$ and it is being pulled by an effective velocity $v_q$. The general solution for the amplitudes $x_q$ in the laboratory reference frame is given by

$$x_q(t) = x_q^0 \cos(\omega_q t) + \left(p_q^0 - v_q\right) \sin(\omega_q t) + v_q t, \tag{3.18}$$

where $x_q^0 = x_q(t=0)$ and $p_q^0 = p_q(t=0)$. The total work done on the polymer during this process is

$$W = \sum_q W_q, \tag{3.19}$$

where $W_q$ is the work performed on the $q$th oscillator. Each $W_q$ has a Gaussian distribution. Thus, $W$ is also a Gaussian distribution with $\mu = \sum_{q=1}^{N} \mu_q$ and $\sigma^2 = \sum_{q=1}^{N} \sigma_q^2$. Thus, using the results for a simple harmonic oscillator (3.8) we get

$$\mu(t) = \frac{1}{2}\sigma^2(t) = 2\sum_{q=1}^{N} v_q^2 \sin^2\left(\frac{\omega_q t}{2}\right). \tag{3.20}$$

Substituting $\omega_q$ and $v_q$ according (3.17) and (3.14) gives

$$\mu(t) = \sum_{q=1}^{N} \frac{v^2}{N+\frac{1}{2}} \cot^2\left(\frac{\alpha_q}{2}\right) \sin^2\left[t\sin\left(\frac{\alpha_q}{2}\right)\right] \tag{3.21}$$

For $N \gg 1$ and $q \ll N$, we find that $\alpha_q \ll 1$. Thus, we can approximate $\sin\left(\frac{\alpha_q}{2}\right) \approx \frac{\alpha_q}{2}$, and $\cot\left(\frac{\alpha_q}{2}\right) \approx \frac{2}{\alpha_q}$ and get

$$\mu(t) \approx \sum_{q=1}^{N} \frac{v^2}{N+\frac{1}{2}} \left(\frac{2}{\alpha_q}\right)^2 \sin^2\left(\frac{\alpha_q}{2}t\right) \tag{3.22}$$

$$= \sum_{q=1}^{N} \frac{v^2}{N+\frac{1}{2}} \left(\frac{2}{\alpha_q^2}\right) [1-\cos(\alpha_q t)] \tag{3.23}$$

$$= \sum_{q=1}^{N} 2v^2 \frac{N+\frac{1}{2}}{\left[\pi(q-\frac{1}{2})\right]^2} \left\{1-\cos\left[\frac{\pi(q-\frac{1}{2})}{N+\frac{1}{2}}t\right]\right\}. \tag{3.24}$$

Since this approximation is valid only for $q \ll N$, it will stop working after long time $t \gg N$. Now we define *scaled mean work*

$$M^*(t) \equiv \frac{\mu(t)}{N+\frac{1}{2}}, \tag{3.25}$$

and *scaled time*

$$t^* \equiv \frac{t}{N+\frac{1}{2}}. \tag{3.26}$$

By taking the limit $N \to \infty$ we obtain

$$M^*(t^*) \approx \frac{2v^2}{\pi^2} \sum_{q=1}^{\infty} \frac{1}{\left(q-\frac{1}{2}\right)^2} - \frac{2v^2}{\pi^2} \sum_{q=1}^{\infty} \frac{4}{(2q-1)^2} \cos\left[\frac{2\pi(2q-1)}{4}t^*\right]. \tag{3.27}$$

With the use of the identity

$$\sum_{q=1}^{\infty} \frac{1}{\left(q-\frac{1}{2}\right)^2} = \frac{\pi^2}{2}, \tag{3.28}$$

we find

$$M^*(t^*) \approx v^2 - \frac{2v^2}{\pi^2} \sum_{q=1}^{\infty} \frac{4}{(2q-1)^2} \cos\left[\frac{2\pi(2q-1)}{4}t^*\right]. \tag{3.29}$$

This is exactly the Fourier series of a triangle wave[1] with an amplitude of $2v^2$ and period time of $T^* = 4$. Let $\Lambda_T(t)$ denote a triangle wave with an amplitude 1 and

[1]The Fourier series of a triangle wave with an amplitude $A$ and period time $T$ is given by: $f(t) = \frac{A}{2} - \frac{A}{\pi^2} \sum_{q=1}^{\infty} \frac{4}{(2q-1)^2} \cos\left(\frac{2\pi(2q-1)}{T}t\right)$

period time $T$. In this notation

$$M^*(t^*) \approx 2v^2\Lambda_4(t^*), \tag{3.30}$$

or, in the original variables

$$\mu(t) \approx 2Nv^2\Lambda_{4N}(t). \tag{3.31}$$

Notice, that this approximation is not valid anymore when $t \gg N$.

Figure 3.2 depicts two different plots of $\mu$ versus time for different $N$s. The system has a period which corresponds to the lowest frequency $T = 2\pi/\omega_{q=1} \approx 4N$. To find the critical velocity $v_c$ we demand that $\mu \ll \sigma$. Using the fact that $\mu = \frac{1}{2}\sigma^2$

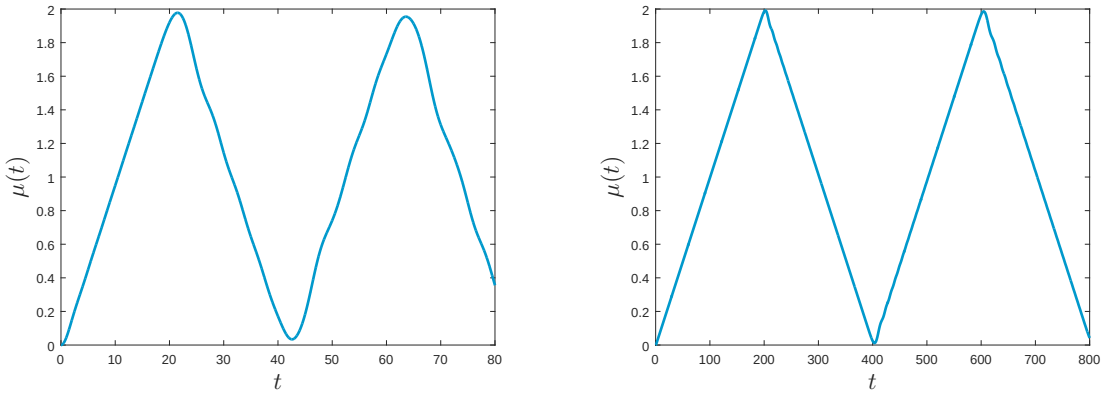


(a) $N = 10$ (b) $N = 100$

**Figure 3.2:** The mean work $\mu = \langle W \rangle$ for $v = 1$ and for polymer of length (a) $N = 10$ (b), $N = 100$. When $N$ grows, $\mu$ more resembles a triangular wave.

this condition becomes $\mu \ll 2$. For $N \gg 1$, we know that $\mu \approx 2Nv^2$, and therefore

$$v_c \approx \frac{1}{\sqrt{N}}. \tag{3.32}$$

Notice, that if we measure the velocity in relative units $u \equiv v/v_c$, and the total pulling length in units of a mean square polymer size $\ell \equiv L/\sqrt{N}$, we find that for fixed $u$ and $\ell$ the distribution $P(W)$ is independent of $N$ (for $N \gg 1$).

### Numerical Results

In order to demonstrate the existence of a critical velocity, we performed $10^3$ simulations of dragging a polymer in free space, with initial conditions chosen from a

canonical distribution. At each simulation the end of the polymer is being dragged along a distance $L = \sqrt{N}$, i.e., $\ell = 1$. The choice of $L = \sqrt{N}$ anticipates the need that arises later in this work, when we will consider the case of a polymer which is being dragged away from a wall. In this case, the pulling length will be more important, where on one hand we need $L$ to be larger than $\sqrt{N}$, but on the other hand being as small as possible. We calculated the work $W$, and built a histogram representing $P(W)$. More details on the specific numerical method that we used can be found in Appendix C.

Figure 3.3 depicts the calculation of the area under $f(W) = e^{-W}P(W)$, which enables calculation of $\Delta F$, for different velocities. Since $\mu \sim v^2$ and $\sigma \sim v$, large velocity means large separation between $f(W)$ and $P(W)$. As we can see, when $v > v_c$ the reconstruction is poor.

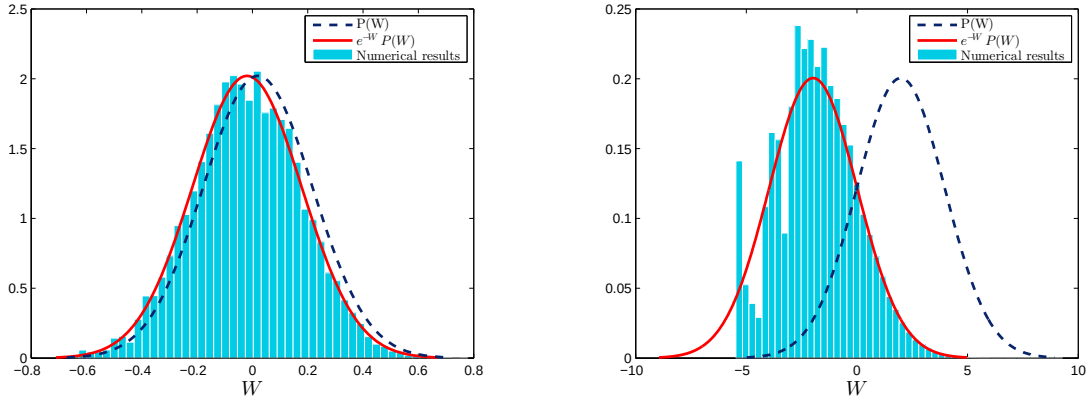


(a) $v = 0.1v_c$ (b) $v = 2v_c$

**Figure 3.3:** The dashed line depicts the theoretical distribution function $P(W)$. The red line depicts the shifted function $f(W) = e^{-W}P(W)$, which was calculated numerically using $10^3$ different initial states. The polymer of size $N = 100$ is being dragged along distance $vt = \sqrt{N}$. The dashed line depicts the theoretical value of $P(W)$, while the red line shows the theoretical curve $f(W)$. The histogram is a numerical reconstruction of $f(W)$. As expected, the reconstruction of the area under $f(W)$ is poor when $v > v_c$.

Figure 3.4 depicts the probability distribution of $W$ for different $N$ while $u = v/v_c = \text{const}$. As has been expected from our theoretical treatment, the shape of the distribution does not depend on $N$ for fixed $u$.

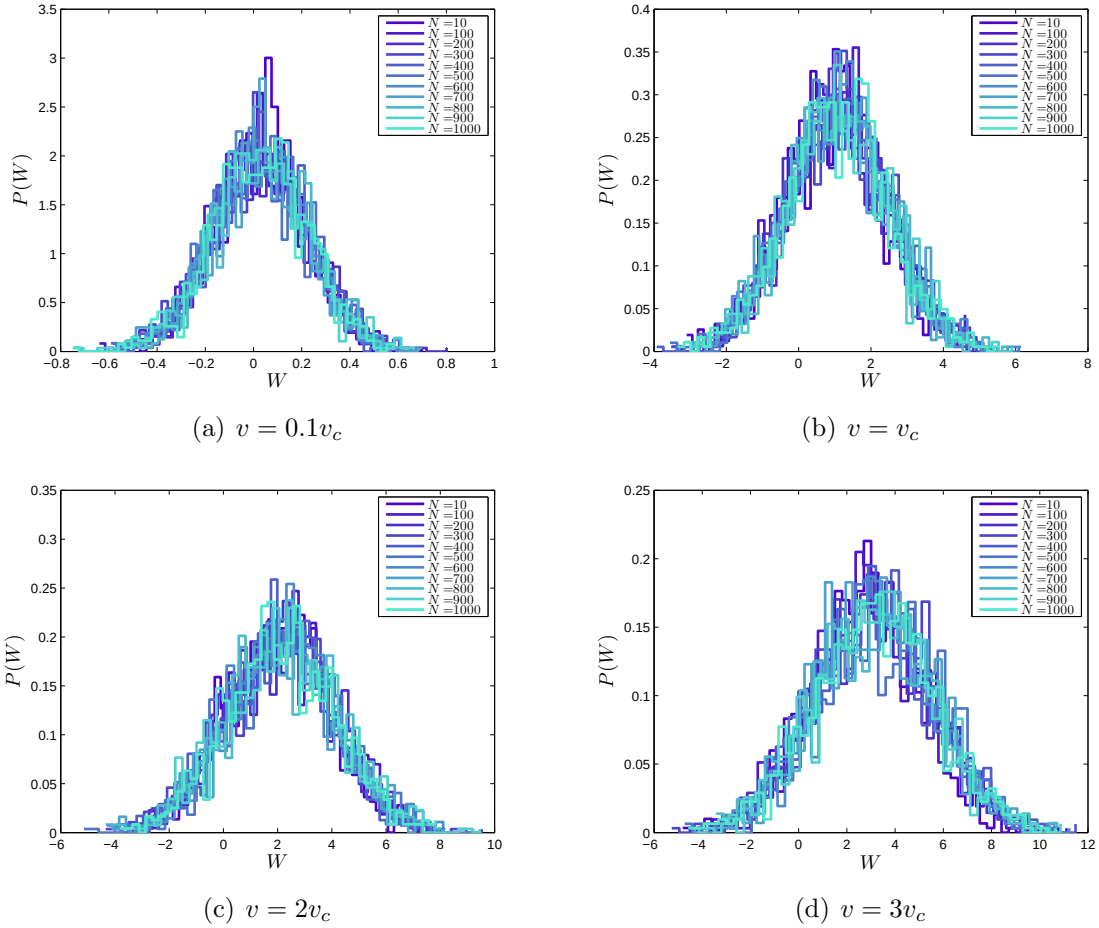


(a) $v = 0.1v_c$ (b) $v = v_c$

(c) $v = 2v_c$ (d) $v = 3v_c$

**Figure 3.4:** Probability distribution $P(W)$ of work for a polymer that is being dragged along distance $vt = \sqrt{N}$ at different velocities. The histogram has been constructed from $10^3$ separate numerical simulations. We can see that for same $u = v/v_c$, $P(W)$ has no dependence on $N$, as has been expected.

## 3.2 Overdamped Langevin dynamics

In this section we consider a Gaussian chain which is dragged in a very viscous fluid. In such a case its dynamics governed by the overdamped Langevin equation (where the inertia term can be neglected). The chain is initially in equilibrium and remains coupled to a thermal bath during the entire process. Our calculation of the work resembles [37–40] where $P(W)$ was calculated for an ideal polymer being stretched.

### 3.2.1 Single oscillator

A harmonic oscillator controlled by Langevin equation was one of the first systems used to demonstrate the Jarzynski equality [41]. There is an extensive theoretical and experimental literature on the subject. Theoretical treatment of a dragged Brownian particle [42] followed an experimental study of translation of a particle in an optical harmonic trap [43], in order to test the violation of the second law of thermodynamics. Other works included a driven harmonic oscillator [44], as well as oscillator subjected to an external non-thermal Gaussian noise [45]. The application of Jarzynski equality was also demonstrated by experiments on harmonic oscillator with varying force constant [24, 25]. A particle that is dragged in a more general potential was also studied [46, 47].

In our case, we consider a particle of mass $m$ moving in a potential created by a spring with force constant $k$ attached to a point $x_0$ which is moving with velocity $v$, i.e., at time $t$ we have $x_0 = vt$. If this motion is in a viscous liquid and under an influence of a thermal noise, it can be described by Lagevin [6] equation

$$m\ddot{x}_1 = -k(x_1 - vt) - m\gamma\dot{x}_1 + R(t), \tag{3.33}$$

where $\gamma$ is a friction constant, while $R(t)$ represents a temperature-depended noise that satisfies

$$\langle R(t)\rangle = 0 \quad ; \quad \langle R(t)R(t')\rangle = 2\gamma k_{\mathrm{B}}T\delta(t-t') \ , \tag{3.34}$$

where $\langle\cdots\rangle$ denotes an average over ensemble of thermal noise. When the friction is strong, the particle loses its momentum at very short times and for such *overdamped* motion the inertia term on the left-hand-side of the equation can be chopped.

As in the Newtonian case, we can use dimensionless variables. The friction constant $\gamma$ and the force constant $k$ define relaxation time $\tau = \gamma/k$, which can be used to

define dimensionless time $t/\tau \to t$. As in the Newtonian case, we will use $k_{\rm B}T$ as an energy unit that can be used to define dimensionless distance $\sqrt{\frac{k}{k_{\rm B}T}}x \to x$, as well as dimensionless velocity $\tau\sqrt{\frac{k}{k_{\rm B}T}}v \to v$. In these units the overdamped Langevin equation becomes

$$\dot{x}_1 = -(x_1 - vt) + R(t), \tag{3.35}$$

where the random thermal force in the dimensionless units satisfies

$$\langle R(t)\rangle = 0 \quad ; \quad \langle R(t)R(t')\rangle = 2\delta(t-t') \ . \tag{3.36}$$

In the reference frame moving at velocity $v$, $\tilde{x}_1 = x_1 - vt$, and equation (3.35) looks even simpler

$$\dot{\tilde{x}}_1 = -\tilde{x}_1 - v + R(t). \tag{3.37}$$

By multiplying both sides of the equation by $e^t$, we get

$$\frac{\mathrm{d}}{\mathrm{d}t}\left[e^t\tilde{x}_1\right] = \left(R(t) - v\right)e^t, \tag{3.38}$$

which can be integrated to obtain

$$\tilde{x}_1(t) = \tilde{x}_1^0 e^{-t} + e^{-t}\int_0^t \big(R(t') - v\big)e^{t'}dt'. \tag{3.39}$$

In these dimensionless units $\tilde{x}_1$ is the stretching of the spring, and $-\tilde{x}_1$ is the force that needs to be applied on the spring to keep it moving with constant velocity $v$ (in the laboratory frame). The force in the laboratory frame is the same as in the moving frame and therefore, the work performed on the system during time $t$ is simply

$$W(t) = -v\int_0^t \tilde{x}_1(t')dt'. \tag{3.40}$$

As seen in (3.39), $\tilde{x}_1(t)$ is a sum of Gaussian variables. Therefore, $\tilde{x}_1(t)$ is a Gaussian variable. Thus, the work $W$ is also a Gaussian variable. In order to find the distribution of work $P(W)$ we only need to find $\mu\big\langle W\big\rangle$ and $\sigma^2 = \big\langle W^2\big\rangle - \big\langle W\big\rangle^2$. These, will define the distribution

$$P(W) = \frac{1}{\sqrt{2\pi\sigma^2}}\exp\left(\frac{-(W-\mu)^2}{2\sigma^2}\right). \tag{3.41}$$

From (3.40) we can calculate:

$$\langle W \rangle = -v \int_0^t \langle \tilde{x}_1(t') \rangle dt' = v^2 \big(e^{-t} + t - 1\big), \tag{3.42}$$

and

$$\langle W^2 \rangle = v^2 \int_0^t \int_0^t \langle \tilde{x}_1(t') \tilde{x}_1(t'') \rangle dt' dt'' = v^4 \big(e^{-t} + t - 1\big)^2 + 2v^2 \big(e^{-t} + t - 1\big). \tag{3.43}$$

So the mean and the variance of the distribution are given by

$$\mu = \langle W \rangle = v^2 \big(e^{-t} + t - 1\big), \tag{3.44}$$

$$\sigma^2 = \langle W^2 \rangle - \langle W \rangle^2 = 2v^2 \big(e^{-t} + t - 1\big). \tag{3.45}$$

We can see again that $\mu$ and $\sigma$ are related in such a way that (2.14) produces $\Delta F = 0$ since $\mu = \frac{1}{2}\sigma^2$.

### 3.2.2 1D polymer

The same Gaussian chain as in subsection 3.1.2 is now moved in a very viscous fluid. In the reference frame moving with velocity $v$, the equations of motion in the dimensionless variables (as defined in the previous sub-section) for $1 \leq n \leq N-1$ are

$$\dot{\tilde{x}}_n = -2\tilde{x}_n + \tilde{x}_{n+1} + \tilde{x}_{n-1} + R_n(t) - v, \tag{3.46}$$

and for $n = N$

$$\dot{\tilde{x}}_n = -\tilde{x}_n + \tilde{x}_{n-1} + R_n(t) - v, \tag{3.47}$$

where $\tilde{x}_n = x_n - vt$ is the location of the $n$th monomer in the moving reference frame, and $R_n(t)$ is the random force acting on the $n$th monomer, which satisfies

$$\langle R_n(t) \rangle = 0 \quad ; \quad \langle R_n(t) R_m(t') \rangle = 2\delta_{n,m}\delta(t - t') \ . \tag{3.48}$$

Again, the system can be decomposed into $N$ eigenmodes by performing a discrete sine Fourier transform that fulfills the boundary conditions,where one end of the polymer is moving with constant velocity $x_0 = vt$, and the other end is free. This way, the Gaussian chain is simply decomposed into $N$ overdamped harmonic oscillators

(as shown in Appendix B). Each oscillator has decay time

$$\tau_q = \frac{1}{4}\sin^{-2}\left(\frac{\alpha_q}{2}\right), \tag{3.49}$$

and is pulled by an effective velocity

$$v_q = \frac{1}{2}Av^2\cot\left(\frac{\alpha_q}{2}\right), \tag{3.50}$$

where

$$A = \sqrt{\frac{2}{N+\frac{1}{2}}} \quad ; \quad \alpha_q = \frac{\pi(q-\frac{1}{2})}{N+\frac{1}{2}} \ . \tag{3.51}$$

The work done on the whole polymer is sum of works performed on each one of the eigenmodes, which are simply dragged oscillators

$$W = \sum_{q=1}^{N} W_q. \tag{3.52}$$

We have already calculated the distribution of work done on a single oscillator, and therefore

$$\mu_q(t) = \frac{1}{2}\sigma_q^2 = \tau_q v_q^2\Big(e^{-\frac{t}{\tau_q}} + \frac{t}{\tau_q} - 1\Big). \tag{3.53}$$

Since $W_q$ has a Gaussian distribution, $W$ has also a Gaussian distribution with mean $\mu = \sum_{q=1}^{N}\mu_q$ and variance $\sigma^2(t) = \sum_{q=1}^{N}\sigma_q^2$, so that

$$\mu(t) = \frac{1}{2}\sigma^2(t) = \sum_{q=1}^{N}\tau_q v_q^2\Big(e^{-\frac{t}{\tau_q}} + \frac{t}{\tau_q} - 1\Big). \tag{3.54}$$

We can examine the mean work for short times and long times, where short or long is relatively to typical time-scales of the system - the relaxation times (3.49). For $q = N$ (3.49) yields the shortest relaxation time of the system

$$\tau_{\min} = \tau_{q=N} = \frac{1}{4}\sin^{-2}\left[\frac{\pi\big(N-\frac{1}{2}\big)}{2\big(N+\frac{1}{2}\big)}\right] \xrightarrow[N\gg 1]{} \frac{1}{4}. \tag{3.55}$$

That is to say, that the shortest time-scale $\tau_{\min}$ of the system is of order unity. The

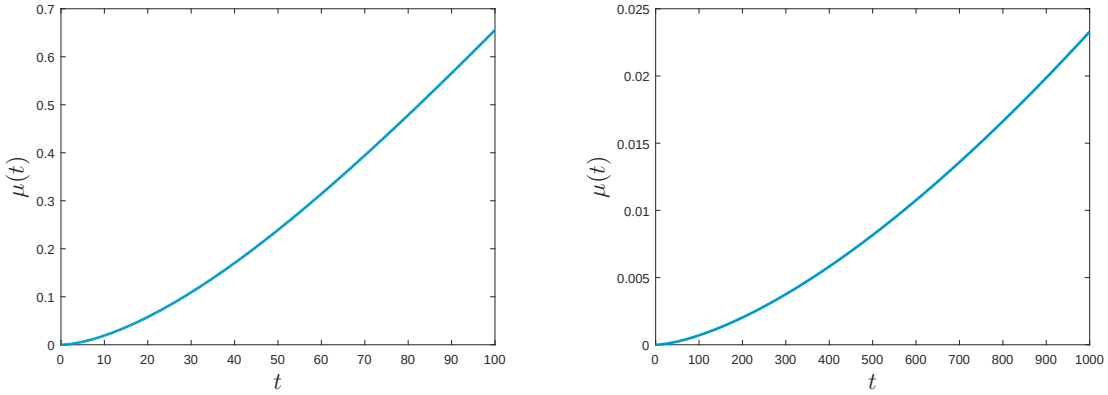


(a) $N = 10$ (b) $N = 100$

**Figure 3.5:** The mean work $\mu = \langle W \rangle$ for $v = 1$ and for polymer of length (a) $N = 10$, and (b) $N = 100$.

largest time scale $\tau_{\max}$ of the system can be obtained by taking $q = 1$ and get

$$\tau_{\max} = \tau_{q=1} = \frac{1}{4}\sin^{-2}\left(\frac{\pi}{4N+2}\right) \xrightarrow[N\gg 1]{} \frac{4}{\pi^2}N^2. \tag{3.56}$$

Thus, the largest time-scale of the system $\tau_{\max} \sim N^2$.
For $t \ll \tau_{\min}$, we can expand the exponential in (3.54) to quadratic order to obtain

$$\mu(t) \approx \sum_{q=1}^{N} \tau_q v_q^2 \Big(1 - \frac{t}{\tau_q} + \frac{1}{2}\Big(\frac{t}{\tau_q}\Big)^2 + \frac{t}{\tau_q} - 1\Big) = \left(\frac{1}{2}\sum_{q=1}^{N}\frac{v_q^2}{\tau_q}\right)t^2. \tag{3.57}$$

By substituting the values of $\tau_q$ from (3.49) and $v_q$ from (3.50) we find

$$\sum_{q=1}^{N}\frac{v_q^2}{\tau_q} = \sum_{q=1}^{N}\frac{1}{4}v^2A^2\cot^2\left(\frac{\alpha_q}{2}\right)\sin^2\left(\frac{\alpha_q}{2}\right) = v^2A^2\sum_{q=1}^{N}\cos^2\left(\frac{\alpha_q}{2}\right) = v^2, \tag{3.58}$$

leading to quadratic behavior

$$\mu(t \ll \tau_{\min}) \approx \frac{v^2}{2}t^2. \tag{3.59}$$

Figure 3.5 shows plots of $\mu$ versus time for different $N$s. We can see that for short times $\mu$ has a parabolic behavior. Notice, that the expression for $\mu$ for short times has no dependence on $N$, because the first monomer still "does not know" it is

connected to a large chain.

For $t \gg \tau_{\max}$ we can drop the exponent in (3.54) and get

$$\mu(t) \approx \left( \sum_{q=1}^{N} v_q^2 \right) t - \mathcal{G}(N), \tag{3.60}$$

where $\mathcal{G}(N) = \sum_{q=1}^{N} \tau_q v_q^2$ and $\sum_{q=1}^{N} v_q^2 = Nv^2$. In order to estimate the dependence of $\mathcal{G}(N)$ on $N$, we can approximate the sum to an integral by taking the limit of $N \gg 1$ and defining a new variable $\zeta = \frac{\pi q}{2N}$

$$\begin{aligned} \mathcal{G}(N) &\approx \frac{v^2}{8N} \sum_{q=1}^{N} \frac{\cot^2\left(\frac{\pi q}{2N}\right)}{\sin^2\left(\frac{\pi q}{2N}\right)} && (3.61) \\ &\approx v^2 \int_{\zeta=\frac{\pi}{2N}}^{\frac{\pi}{2}} \frac{\cot^2\zeta}{\sin^2\zeta} d\zeta && (3.62) \\ &\approx v^2 \cot^3\left(\frac{\pi}{2N}\right). && (3.63) \end{aligned}$$

By approximating $\cot(\pi/2N) \approx N$ we obtain

$$\mathcal{G}(N) \approx v^2 N^3. \tag{3.64}$$

Thus, for $t \gg \tau_{\max}$, i.e., $t \gg N^2$, $\mathcal{G}(N)$ can be neglected and $\mu(t)$ is given by

$$\mu(t \gg \tau_{\max}) \approx Nv^2 t, \tag{3.65}$$

and we get a linear dependence on $t$ for $t \gg \tau_{\max}$, as shown in Figure 3.5.

To find the critical pulling velocity we will focus on the large times regime. Suppose we drag the chain along distance $L = vt \sim \sqrt{N}$, then using condition (2.15), we get

$$\mu \approx N^{\frac{3}{2}} v < 1, \tag{3.66}$$

which defines the critical velocity

$$v_c \approx N^{-3/2}. \tag{3.67}$$

Again, for $N \gg 1$, one can define new relative velocity $u = v/v_c$ and relative distance

$\ell = vt/\sqrt{N}$ such that the distribution of work $P(W)$ will be independent of the chain size $N$ for fixed $u$ and $\ell$. In these variables, the distribution of work for $t \gg \tau_{\max}$ is simply a Gaussian with mean and variance

$$\mu = \frac{1}{2}\sigma^2 \sim u\ell. \tag{3.68}$$

Notice that in this case our ability to reconstruct $\Delta F$ correctly also depends on the pulling length $\ell$ (or pulling time). Unlike the Newtonian dynamics case, where $\mu$ and $\sigma$ were bounded, in this case $\mu \sim \ell$ and $\sigma \sim \sqrt{\ell}$, which means that they are not bounded. At some point $\mu$ will be large enough so that the Gaussian of $P(W)$ will be centered far away from the center of the shifted Gaussian $f(W)$, and there will be no appreciate overlap between them. However, if we drag the polymer a distance which if of order of a few typical polymer sizes ($\ell \sim 1$), the critical velocity defined in (3.67) is still valid.

### Numerical Results

Even though this problem has an analytical solution, we solved the problem numerically to demonstrate the existence of a critical velocity $v_c$. We performed $10^3$ simulations of dragging a Gaussian chain in free space in the presence of a Gaussian noise. We chose $10^3$ different initial states from a canonical distribution, while for each initial state we calculated the work done by dragging the end of the polymer along a distance $L = \sqrt{N}$ with constant velocity $v$. We built the histogram representing $P(W)$, and reconstructed the area under the shifted curve $f(W) = e^{-W}P(W)$. More details on the specific numerical method that we used, can be found in Appendix C.

Figure 3.6 depicts the calculation of the area under $f(W)$ for different velocities. Since $\mu \sim v^2$, large velocity means large separation between $f(W)$ and $P(W)$. As we can see, when $v > v_c$ the reconstruction is poor. In Figure 3.7 we can see the numerical calculation of $P(W)$ for different $N$ while the variables $u$ and $\ell$ remain constant. As derived in (3.68), the distributions are independent of $N$ for fixed $u$ and $\ell$.

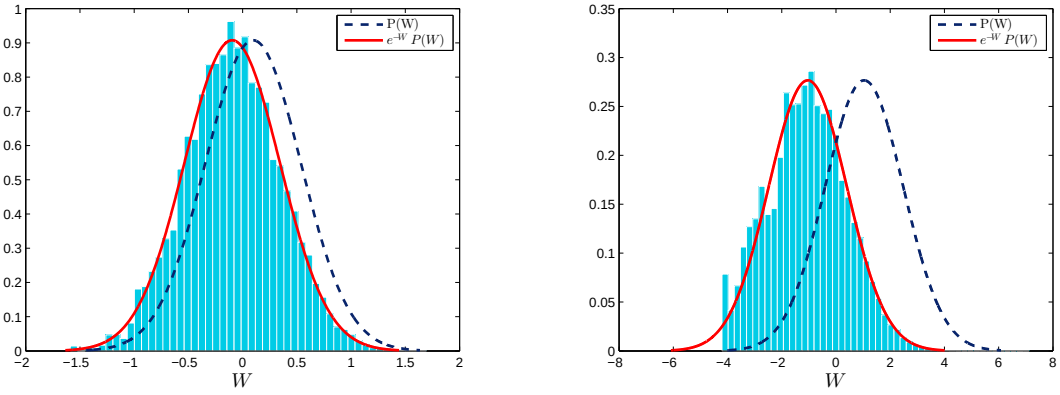


(a) $v = 0.1v_c$ (b) $v = 2v_c$

**Figure 3.6:** The dashed line depicts the theoretical distribution function $P(W)$. The red line depicts the shifted function $f(W) = e^{-W}P(W)$, which was calculated numerically using $10^3$ different initial states. The polymer of size $N = 100$ is being dragged along distance $vt = \sqrt{N}$. The dotted line depicts the theoretical value of $P(W)$, while the red line shows the theoretical curve $f(W)$. The histogram is a numerical reconstruction of $f(W)$. As expected, the reconstruction of the area under $f(W)$ is poor when $v > v_c$.

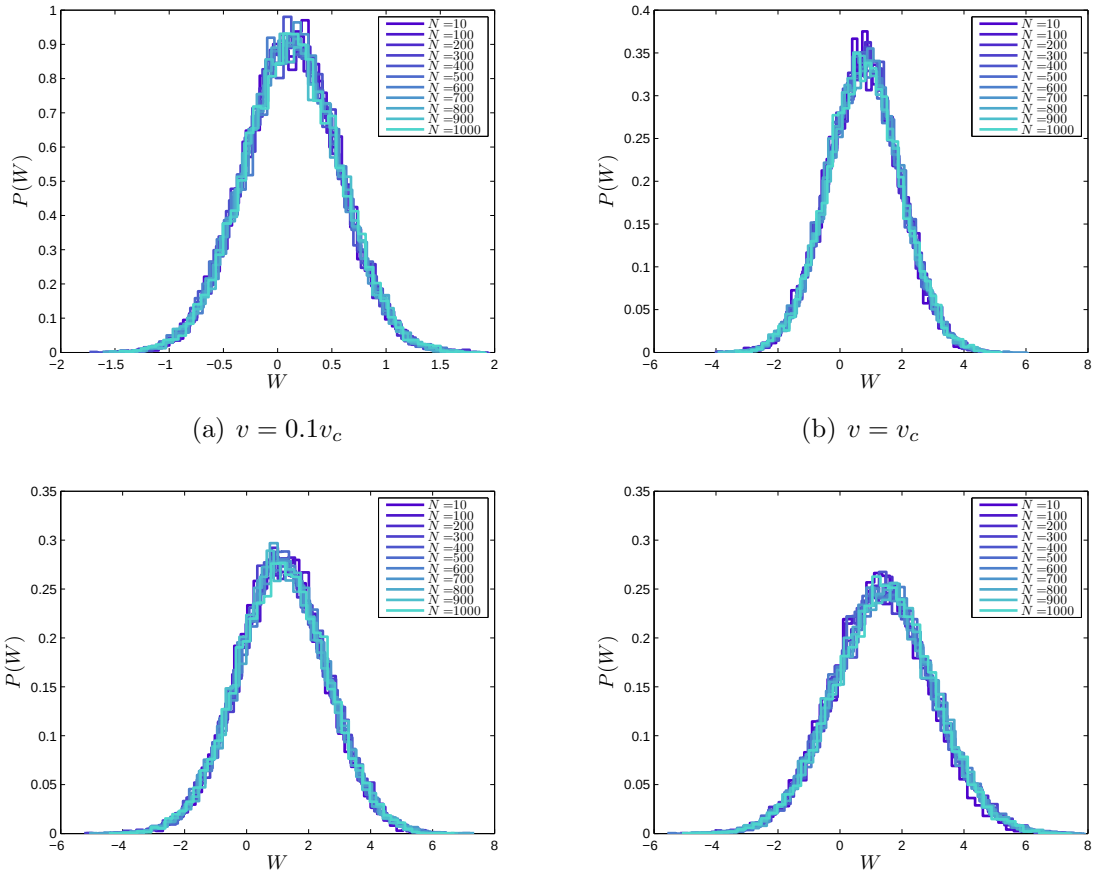


(a) $v = 0.1v_c$ (b) $v = v_c$

(c) $v = 2v_c$ (d) $v = 3v_c$

**Figure 3.7:** Probability distribution of work for the overdamped Langevin dynamics case. The polymer is being dragged along distance $vt = \sqrt{N}$ with different velocities. We can see, that for $u = v/v_c = \text{const.}$, $P(W)$ is independent $N$.

# Chapter 4

# Dragging a Polymer Away from a Wall

In this chapter we deal with the problem of an ideal polymer which is initially located near a wall, and is being dragged far away from the wall. We would like to use the Jarzynski equality to calculate the free energy difference $\Delta F$ between the initial equilibrium state (the polymer near the wall) and the final equilibrium state (the polymer far away from the wall). This non-equilibrium problem has no analytical solution. The distribution of work is generally no longer a Gaussian and $\Delta F$ is no longer zero. We find the critical velocities using qualitative arguments, and compare them with numerical results. We considered both for Newtonian dynamics (ND) and overdamped Langevin dynamics (OLD) cases.

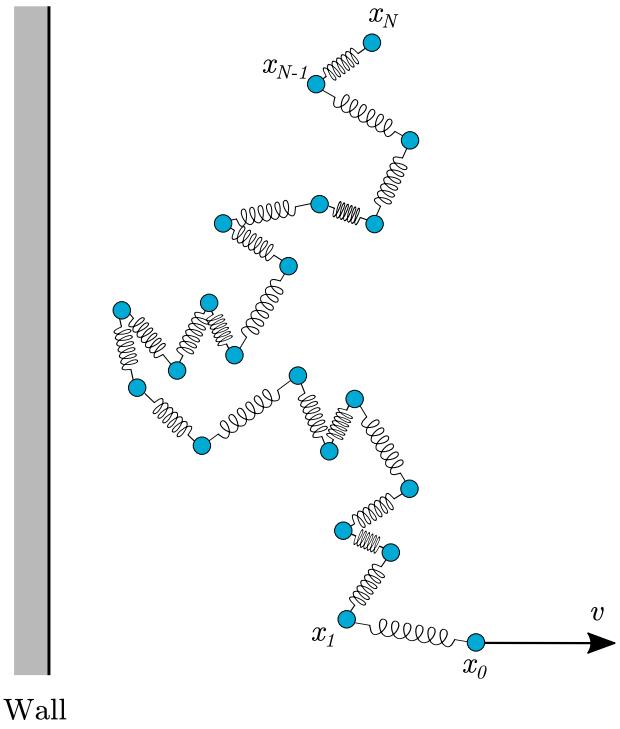


**Figure 4.1:** A Gaussian chain near a wall, while its end is dragging away from the wall with constant velocity $v$ and the other end is free. Notice, that we consider only 1D Gaussian chains, and the second dimension is for illustration only.

## 4.1 Adiabatic motion of a single oscillator

Consider the single oscillator system described in Sec. 3.1.1 with a wall added at $x = 0$, so we have a particle which is initially attached by a spring to a rigid wall. The oscillator can collide elastically with the wall, which means the wall can change the momentum of the oscillator but not its energy. Now we start moving away the point $x_0$, to which the spring is attached, away from the wall. The Hamiltonian of the system is

$$\mathcal{H} = \frac{1}{2}p_1^2 + \frac{1}{2}(x_1 - x_0)^2 + V_{\text{wall}}(x_1), \tag{4.1}$$

where $x_0 = vt$, and $V_{\text{wall}}$ is the wall potential

$$V_{\text{wall}}(x_1) = \begin{cases} 0, & x_1 > 0, \\ \infty, & x_1 < 0. \end{cases} \tag{4.2}$$

As long as the particle does not touch the wall, its motion is described by

$$x_1(t) = x_1^0 \cos(t) + (p_1^0 - v)\sin(t) + vt. \tag{4.3}$$

When the particle hits the wall, its velocity is reversed. Thus, the particle's movement will be divided into collisionless segments, separated by the points when the particle collides the wall, as depicted in Figure 4.2. Each segment is described by

$$x_n(t) = x_{0_n} \cos(t) + (p_{0_n} - v)\sin(t) + vt, \tag{4.4}$$

where $t_{n-1} < t < t_n$ for the $n$th segment, and $(x_{0_n}, p_{0_n})$ are the initial conditions (at $t = 0$) of the $n$th segment. When the trajectory of the oscillator in the phase space is closed, we can define an *adiabatic invariant* $\mathcal{I}$ [48], which is the area enclosed by the trajectory in the phase space

$$\mathcal{I} = \oint p_1 dx_1. \tag{4.5}$$

Generally, the trajectories of the oscillator in phase space are not closed. However, if the particle is dragged sufficiently slow, i.e., during one period of the oscillator we barely change the zero point $x_0$, the trajectories are almost closed, as demonstrated in Figure 4.3. It can be shown [48], that the lowest order non-vanishing term in the

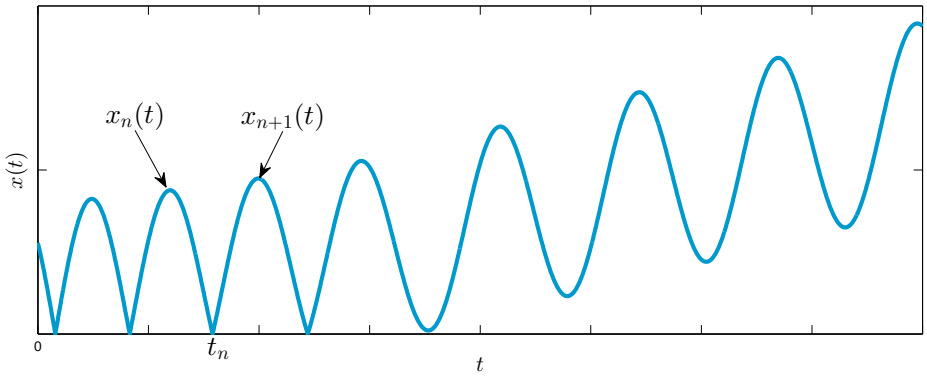


**Figure 4.2:** An example of a path of a particle attached by a linear harmonic spring to a point initially equilibrated near a wall as it is dragged away from the wall.

change of the adiabatic invariant $\mathcal{I}$ is $v^2$, i.e.,

$$\frac{\mathrm{d}\mathcal{I}}{\mathrm{d}t} \approx v^2. \tag{4.6}$$

Therefore, for small velocities the change in $\mathcal{I}$ is negligible, and $\mathcal{I}$ is conserved. Using the fact that the area enclosed in the phase space trajectory remains constant we can find the work done on the oscillator. The total energy of the system is

$$E = \frac{1}{2}p_1^2 + \frac{1}{2}(x_1 - vt)^2. \tag{4.7}$$

In the absence of the wall, for constant $E$ and $t$, this represents a circle of a radius $\sqrt{2E}$ in $(x, p)$ plane. In the presence of the wall the circles "trimmed" at $x = 0$. In particular at $t = 0$, when the spring is attached to the wall, the trajectory in the phase space is a semi-circle, with

$$\mathcal{I}_1 = \pi E_1, \tag{4.8}$$

where $E_1$ is the energy of the oscillator at that time. When the oscillator moves away from the wall, its trajectory becomes a complete circle, and the area becomes

$$\mathcal{I}_2 = 2\pi E_2, \tag{4.9}$$

where $E_2$ is the energy of the oscillator after it was pulled away from the wall. Since the area is an adiabatic invariant of the system $\mathcal{I}_1 = \mathcal{I}_2$, we find that for small $v$ the

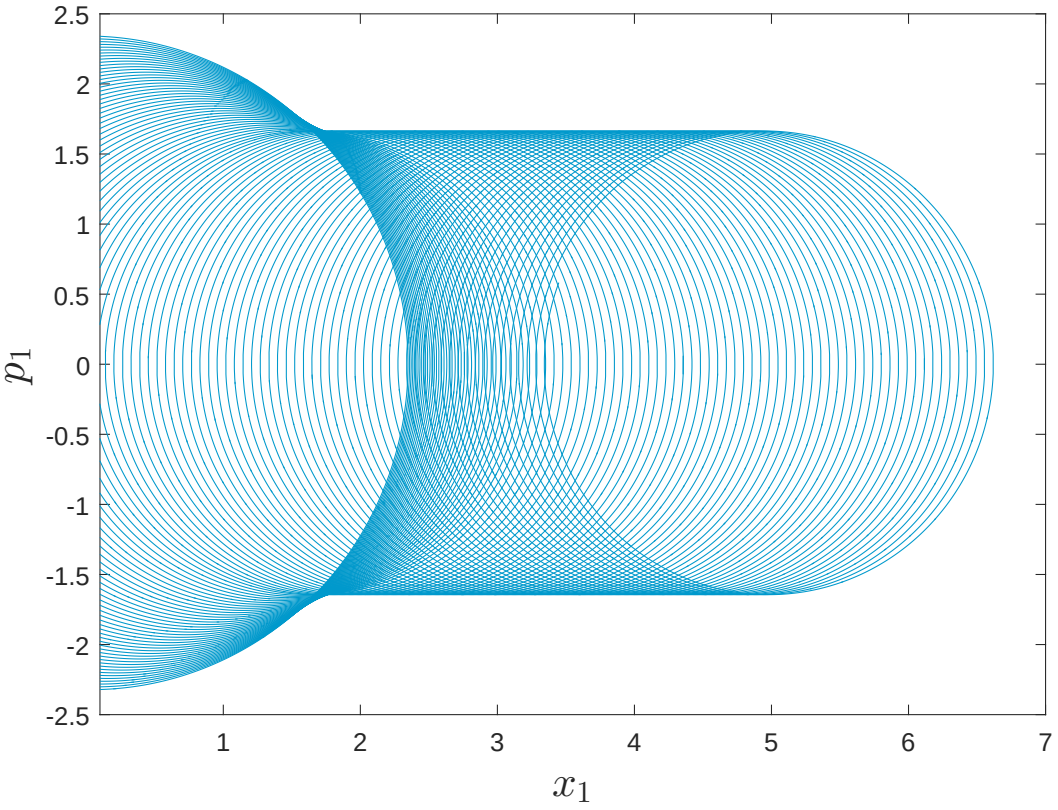


**Figure 4.3:** An example of a possible trajectory in the phase space of an oscillator which is dragged away from the wall with a velocity $v = 0.01$. When the oscillator is attached to the wall the trajectory is half a circle, when it is far away from the wall the trajectory is a complete circle. For an adiabatic movement, each circle is almost closed, and the area enclosed by the trajectory remains constant.

energies are related as $E_1 = 2E_2$. The work done on the oscillator is the difference between the final and initial energy

$$W = E_2 - E_1 = -\frac{E_1}{2}. \tag{4.10}$$

In terms of the initial state $(x_1^0, p_1^0)$ the work is:

$$W(x_1^0, p_1^0) = -\frac{1}{4}\left[\left(x_1^0\right)^2 + \left(p_1^0\right)^2\right]. \tag{4.11}$$

In order to find the distribution of work $P(W)$ we need to calculate the average $\langle \delta\left(W - W\left(x_1^0, p_1^0\right)\right)\rangle$ with respect to the initial Boltzmann distribution of $x_1^0$ and $p_1^0$. The $\delta$ function can be presented as Fourier transform, i.e., $\delta(y) = \frac{1}{2\pi}\int_{-\infty}^{\infty} e^{iky} dk$,

which gives

$$P(W) = \left\langle \delta \left( W - W(x_1^0, p_1^0) \right) \right\rangle = \frac{1}{2\pi} \int_{-\infty}^{\infty} e^{ikW} \langle e^{-ikW(x_1^0, p_1^0)} \rangle dk. \tag{4.12}$$

The thermal average over initial states yields

$$\begin{aligned} \left\langle e^{-ikW(x_1^0, p_1^0)} \right\rangle &= \frac{1}{\pi} \int_{-\infty}^{\infty} \int_{0}^{\infty} e^{-\frac{x^2}{2}\left(1-\frac{ik}{2}\right)} e^{-\frac{p^2}{2}\left(1-\frac{ik}{2}\right)} dx dp \\ &= \frac{2}{2-ik}. \end{aligned} \tag{4.13}$$

By substituting (4.13) into (4.12) we find the probability density function of $W$ in adiabatic process

$$\begin{aligned} P(W) &= \frac{1}{\pi} \int_{-\infty}^{\infty} \frac{e^{ikW}}{2-ik} dk \\ &= 2e^{2W} \theta(-W), \end{aligned} \tag{4.14}$$

where $\theta(x)$ is the Heaviside step function. From the knowledge of $P(W)$, we can reproduce the equilibrium free energy difference of the oscillator. This can be computed with a direct free energy calculation of an oscillator attached to a wall and oscillator in free space. The partition function $Z_{\text{free}}$ of an oscillator in free space is twice larger than the partition function $Z_{\text{wall}}$ of an oscillator attached to a wall, since the wall "trimmed" half of the available states in free space. Thus, the free energy difference $\Delta F$ between the initial state, where the spring is attached to the wall, and final state, where the oscillator is far away from the wall, is given by

$$\Delta F = -\ln \left( \frac{Z_{\text{free}}}{Z_{\text{wall}}} \right) = -\ln(2). \tag{4.15}$$

We can easily check that this distribution indeed reproduces the correct $\Delta F$ using the Jarzynski equality (2.7)

$$\Delta F = -\ln \left( \int_{-\infty}^{0} 2e^{2W} e^{-W} dW \right) = -\ln(2). \tag{4.16}$$

We can also check that $P(W)$ yields the expected mean value of work (4.10), which is minus half of the average total energy $\langle E_1 \rangle = \langle x_0^2/2 \rangle + \langle p_0^2/2 \rangle = 1$

$$\langle W \rangle = \int_{-\infty}^{0} 2We^{2W} dW = -\frac{1}{2} = -\frac{\langle E_1 \rangle}{2}. \tag{4.17}$$

Figure 4.4 shows the comparison between the analytical result and the numerical result.

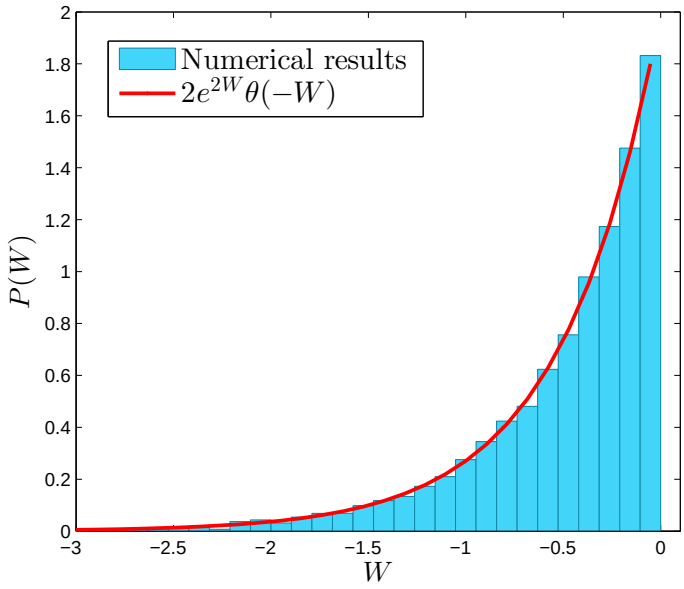


**Figure 4.4:** A numerical reconstruction of $P(W)$ for $v = 0.01$ and $L = vt = 5$. The red line depicts the analytical distribution function (4.14) for adiabatic motion.

## 4.2 Estimation of $v_c$ for 1D polymer

### 4.2.1 Newtonian dynamics

For a reliable reconstruction of the free energy, the polymer should be moved sufficiently slowly. From (1.3) we see that the velocity of the center of mass velocity of the polymer is

$$\mathbf{v}_{\mathrm{cm}} = \frac{1}{N}\sum_{i=1}^{N}\dot{\mathbf{R}}_i. \tag{4.18}$$

For a polymer in free space the average velocity of the center of mass is $\langle \mathbf{v}_{\mathrm{cm}} \rangle = 0$. However, the typical, or the r.m.s velocity $v_{\mathrm{cm}} = \sqrt{\langle \mathbf{v^2}_{\mathrm{cm}} \rangle}$ is

$$v_{\mathrm{cm}} = \sqrt{\frac{1}{N^2}\sum_{i,j=1}^{N}\left\langle \dot{\mathbf{R}}_i \cdot \dot{\mathbf{R}}_j \right\rangle} = \frac{v_{\mathrm{th}}}{\sqrt{N}}, \tag{4.19}$$

where $v_{\mathrm{th}}$ is the typical (thermal) velocity of a single monomer. In our dimensionless units $v_{\mathrm{th}} = 1$ and therefore $v_{\mathrm{cm}} = 1/\sqrt{N}$. The time $t$ it would take the polymer to move its own size $L = \sqrt{N}$, would be $t = L/v = N$. This is also the period of the slowest eigenmode of a free polymer (3.17) [4]. For a free-polymer this can be calculated exactly, but even in presence of a wall, the typical time of overall motion of the polymer would be the same. It is natural to define velocity $v$ of a slow motion, such that during this time the polymer is not dragged more than its own size $L = \sqrt{N}$, i.e., we must require $v < v_{\mathrm{cm}}$. In other words, for the ND case the critical velocity $v_c$ coincides with the typical velocity of the center of mass $v_{\mathrm{cm}}$, or

$$v_c \approx \frac{1}{\sqrt{N}}, \tag{4.20}$$

which coincides with the analytical result (3.32) for the critical velocity in free space.

Possible generalization to non-ideal polymers could be that of self-avoiding-walk (SAW) polymers, where two monomers can no longer occupy the same place in space. The r.m.s end-to-end distance of such a polymer is described by a different exponent $\nu \neq \frac{1}{2}$, i.e., $R \sim N^{\nu}$. We can see that eventually, the size of the polymer has no influence on $v_{\mathrm{cm}}$ as well as on the critical velocity $v_c$. Therefore, the same critical velocity (4.20) will be valid also for SAW polymers.

### 4.2.2 Overdamped Langevin dynamics

The center of mass of an $N$-monomer polymer whose motion is described by Langevin equation in free space performs diffusion, characterized by diffusion constant $D$, which is $N$ times smaller than the diffusion constant $D_0$ of a single monomer. $D_0$ is of order 1 in our dimensionless units. Therefore, the time $t$ it takes it to diffuse its own size $L = \sqrt{N}$, is

$$t \approx \frac{L^2}{D} = \frac{N}{D_0/N} \approx N^2 \tag{4.21}$$

This is also the slowest relaxation time of an internal mode of the polymer.

If the polymer is being dragged with a velocity $v$, we would like it to be sufficiently small, such that during the same time $t$, the distance $vt$ that the polymer is dragged would not exceed its own size $L$. This means that we need $v < N^{-\frac{3}{2}}$, or

$$v_c \approx N^{-\frac{3}{2}}. \tag{4.22}$$

which coincides with the analytical result (3.67) for the critical velocity in free space. The presence of the wall does not significantly modify the natural diffusion of the polymer or its internal relaxation times. Therefore, this $v_c$ is also valid in the presence of the wall. Note, that (4.22) coincides with the exact result (3.67) in free space.

The generalization to SAW polymers for this case, will take into account the size of the polymer $N^\nu$. By replacing $L = N^\nu$, we simply find a general critical velocity

$$v_c \approx N^{-\nu-1}. \tag{4.23}$$

## 4.3 Numerical results

We performed a numerical simulation and found the distribution of work as well as the free energy difference for different velocities and different chain sizes $N$. The numerical methods are detailed in Appendix C. From the numerical results we can deduce properties of such distributions both for Newtonian dynamics (ND) and overdamped Langevin dynamics (OLD). In order to ensure that the polymer is far enough from the wall, the polymer has been dragged away from the wall a distance $L$ which is $\ell = 5$ times the typical size of the polymer $\sqrt{N}$, i.e., $L = \ell\sqrt{N}$. Notice, that this is a non-equilibrium process and the average size of the polymer during the pulling might be grater than $\sqrt{N}$, and that is why we choose $L = 5\sqrt{N}$. We

repeated this process many times with different initial states, chosen from a canonical distribution.

Notice, that in this case the free energy difference $\Delta F$ is no longer zero. As we have already seen in (2.2) and (2.4), we can determine the value of $\Delta F$ up to a constant

$$\Delta F = -\frac{1}{2}\ln N + \mathcal{C}, \tag{4.24}$$

where the value of the constant $\mathcal{C} \approx -0.589$ is calculated numerically in Appendix D. In order to give some quantative measure to the deviation from equilibrium, let us introduce the *dissipative work* [38]

$$W_{\mathrm{d}} = W - \Delta F. \tag{4.25}$$

For isothermal quasi-static processes, the mean work is equal to the free energy difference $\Delta F$. Thus, $W_{\mathrm{d}}$ gives some measure of deviation from quasi-static processes, i.e., an entropy production term.

Generally, the distribution of work $P(W)$ depends on the number of monomers $N$, since the free energy difference is function of $N$. After we numerically calculated the distributions $P(W)$ for for fixed $u = v/v_c$ and $\ell = L/\sqrt{N}$, we noticed that if we subtract the free energy difference from the work, i.e., working with the dissipative work $W_{\mathrm{d}}$, the distribution $P(W_{\mathrm{d}})$ of the dissipative work looks like it has no dependence on $N$.

Figure 4.5 and 4.6 show the histograms of the distributions of the dissipative work $W_{\mathrm{d}}$ for ND and OLD cases, respectively. For each case a comparison has been done between distributions with different polymer sizes $N$, but the same relative velocity $u = v/v_c$. As we can see, for $N \gg 1$ and fixed $u$ and $\ell$ the shape of the distributions looks the same, no matter what is the size of the chain. This result is observed both for ND case and OLD case. Possibly, the fact that the distributions collapse into the same shape, implies of a limiting curve for $N \to \infty$. Since we only deal with $N \leq 100$, we cannot declare this result with a high degree of certainty. Notice, that a similar result was obtained analytically for a polymer in free space. In that case of a polymer in free space, the free energy difference was zero. Thus, $W_{\mathrm{d}} = W$ and $P(W_{\mathrm{d}}) = P(W)$. For the case of a polymer near a wall we have no analytical solution to examine. Still, we can give some qualitative arguments to justify the existence of this property for the case of polymer near the wall:

First, notice that the probability density $P(W_{\mathrm{d}})$ is generally restricted by two

constrains:

1. The probability density $P(W_\mathrm{d})$ must be normalized

$$\int_{-\infty}^{\infty} P(W_\mathrm{d}) dW_\mathrm{d} = 1. \tag{4.26}$$

2. By dividing (2.6) by $e^{-\Delta F}$, we find that the shifted function $f(W_\mathrm{d}) = e^{-W_\mathrm{d}} P(W_\mathrm{d})$ must also be normalized

$$\int_{-\infty}^{\infty} e^{-W_\mathrm{d}} P(W_\mathrm{d}) dW_\mathrm{d} = 1. \tag{4.27}$$

These two constraints somewhat restrict the shape of the distribution. The second constraint means that the are $A_\mathrm{d}$ under $f(W_\mathrm{d}) = e^{-W_\mathrm{d}} P(W_\mathrm{d})$ is $A_\mathrm{d} = 1$.

For the OLD case we know that for small velocities (quasi-static isothermal pulling) the work must be equal to the free energy difference. Also we know that the for large pulling time the polymer can be treated as a polymer in a free space (since its too far from the wall) and the dominant term of the work grows linearly with time (3.65). Combining these two facts together, we get

$$W_\mathrm{OLD} \approx N v^2 t + \Delta F. \tag{4.28}$$

In terms of the pulling distance $L = vt = \ell\sqrt{N}$ and the velocity parameter $u = v/v_c$, we simply get that the dissipative work for the OLD case is independent of $N$

$$W_\mathrm{OLD} - \Delta F \approx u\ell. \tag{4.29}$$

Another important property of the numerically calculated $P(W_\mathrm{d})$ is the tail of the distribution. As we can see that in the ND case (Figure 4.5), the distributions are definitely not symmetric anymore and they have a long tail towards the lower values of $W_\mathrm{d}$. In the OLD case (Figure 4.6) the long tail is absent. This tail has a critical influence on our ability to reconstruct the correct $\Delta F$. Figures 4.7 and 4.8 depict the reconstruction of $\Delta F$ for various velocities and different polymer sizes. The theoretical value of $\Delta F$ was calculated in Appendix D, and it is depicted by the black line. In both cases (ND and OLD) we can see that when $v < v_c$ the free energy

differences that calculated using Jarzynski equality are close to the theoretical value, while for $v > v_c$, the numerical results unable to reproduce the correct values of $\Delta F$. We can also notice that, since the size of the sample is finite, and the number of available configurations grows with $N$, the reconstruction becomes poorer for large $N$.

Notice, that the reconstructed free energy for $v \geq v_c$ is smaller than the expected value for the ND case, and is larger than the expected value for the OLD case. The reason for that is the long tails of the distributions in the ND case, and the absence of the tail in the OLD case. Let us denote by $\tilde{A}_{\rm d}$ the numerically reconstructed area under $f(W_{\rm d})$. Figures 4.9 and 4.10, depict an illustration of this point, i.e., if our sample size is finite, we will never be able to calculate the whole tail numerically. Thus, rare values of work, which are located on the tail of $P(W_{\rm d})$, will be very dominant after multiplying the histogram by $e^{-W_{\rm d}}$. Therefore, $\tilde{A}_{\rm d}$ will be larger than the theoretically expected value, i.e., $\tilde{A}_{\rm d} > 1$ (as shown in Figure 4.9). However, if these rare values of work are absent, the numerically calculated area $\tilde{A}_{\rm d}$ will be smaller than the theoretical expected one, i.e., $\tilde{A}_{\rm d} < 1$ (as shown in Figure 4.10). Let us denote by $\Delta\tilde{F}$ the numerically estimated free energy difference, which is related to $\tilde{A}_{\rm d}$ via (2.7)

$$\Delta\tilde{F} - \Delta F = -\ln\left(\tilde{A}_{\rm d}\right). \tag{4.30}$$

Thus, if $\tilde{A}_{\rm d} > 1$ (as in the ND case) we get $\Delta\tilde{F} < \Delta F$, and if $\tilde{A}_{\rm d} < 1$ (as in the OLD case) we get $\Delta\tilde{F} > \Delta F$.

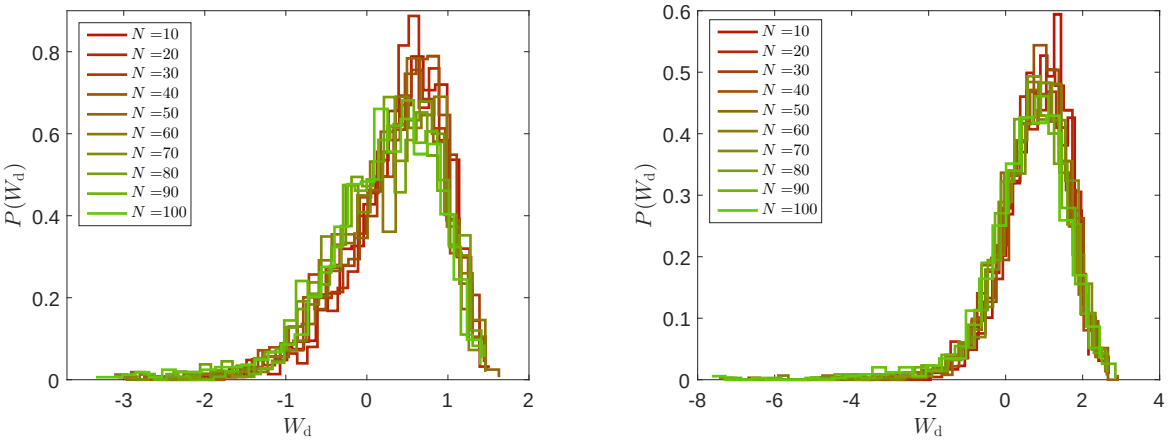


(a) $v = 0.1v_c$ (b) $v = v_c$

(c) $v = 2v_c$ (d) $v = 3v_c$

**Figure 4.5:** Probability density $P(W_\mathrm{d})$ of the dissipative work $W_\mathrm{d}$ for the case of ND. We picked $10^3$ different initial states for each velocity and polymer size. In all of the cases the polymer was dragged a relative distance of $\ell = 5$.

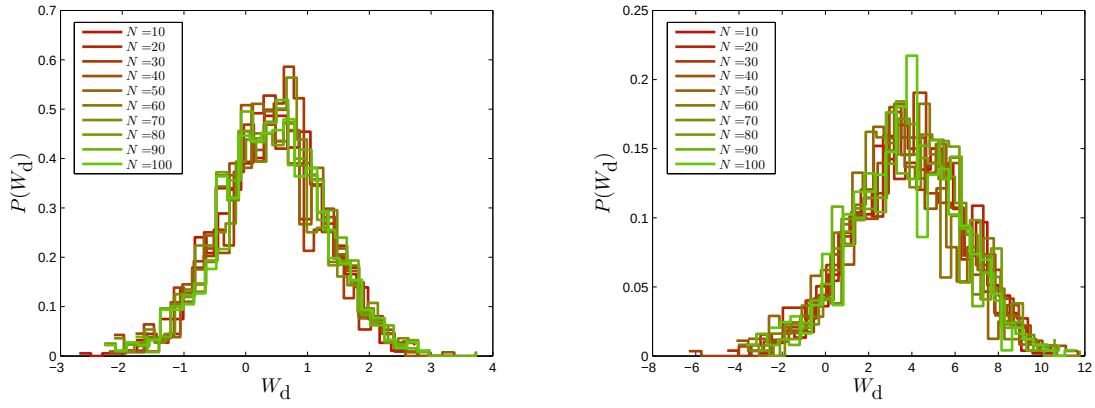


(a) $v = 0.1v_c$ (b) $v = v_c$

(c) $v = 2v_c$ (d) $v = 3v_c$

**Figure 4.6:** Probability density $P(W_d)$ of the dissipative work $W_d$ for the case of OLD. We picked 500 different initial states for each velocity and polymer size. In all of the cases the polymer was dragged a relative distance of $\ell = 5$.

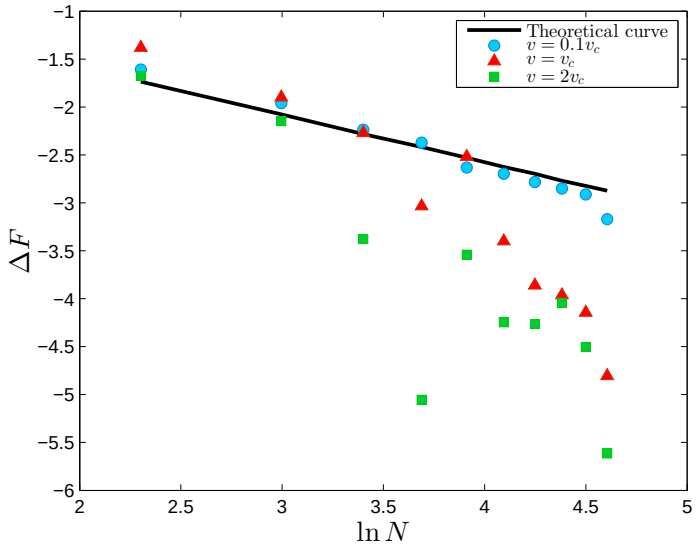


**Figure 4.7:** Reconstruction of $\Delta F$ for different polymer sizes and different velocities in the ND case. The black line depicts the theoretical line as calculates in Appendix D, different colors of dots present different pulling velocity. We can see that the reconstruction becomes poor when $v > v_c$.

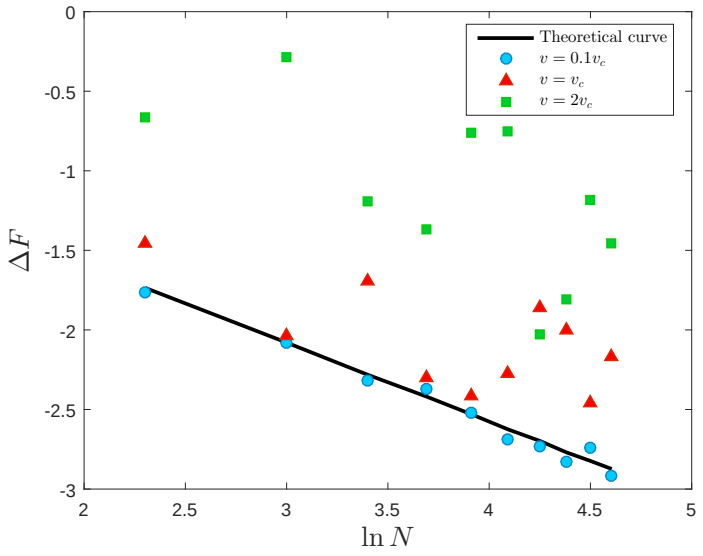


**Figure 4.8:** Reconstruction of $\Delta F$ for different polymer sizes and different velocities in the OLD case. The black line depicts the theoretical line as calculates in Appendix D, different colors of dots present different pulling velocity. We can see that the reconstruction becomes poor when $v > v_c$.

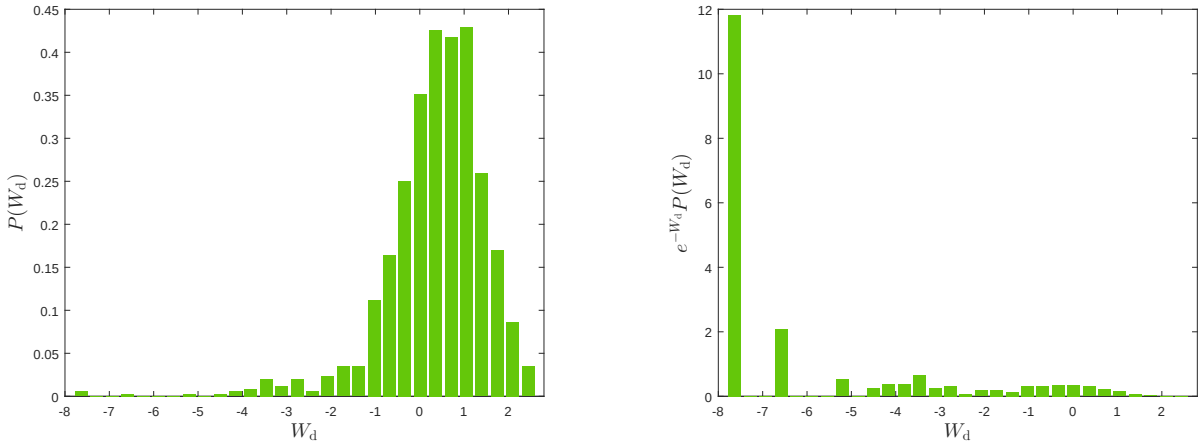


(a) (b)

**Figure 4.9:** Numerical calculation of $P(W_\mathrm{d})$ and $e^{-W_\mathrm{d}}P(W_\mathrm{d})$ for the ND case, where $v = v_c$ and $N = 100$. (a) Histogram of the distribution $P(W_\mathrm{d})$ (b) Histogram of the shifted function $f(W_\mathrm{d}) = e^{-W_\mathrm{d}}P(W_\mathrm{d})$. The numerical value of the area under $f(W_\mathrm{d})$ is $\tilde{A}_\mathrm{d} \approx 120 > 1$.

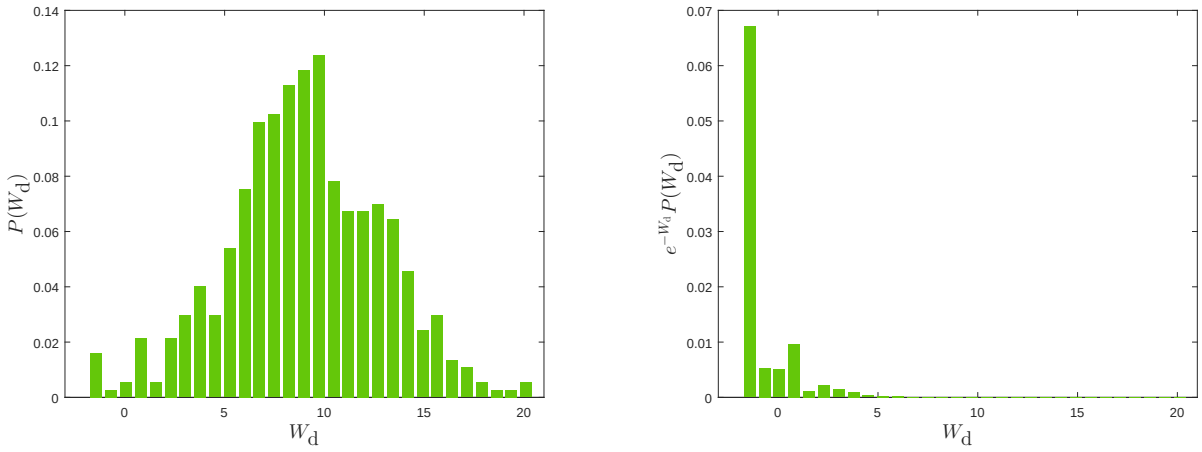


(a) (b)

**Figure 4.10:** Numerical calculation of $P(W_\mathrm{d})$ and $f(W_\mathrm{d}) = e^{-W_\mathrm{d}}P(W_\mathrm{d})$ for the OLD case, where $v = 3v_c$ and $N = 100$. (a) Histogram of the distribution $P(W_\mathrm{d})$ (b) Histogram of the shifted function $f(W_\mathrm{d}) = e^{-W_\mathrm{d}}P(W_\mathrm{d})$. The numerical value of the area under $f(W_\mathrm{d})$ is $\tilde{A}_\mathrm{d} \approx 0.073 < 1$.

# Chapter 5

# Conclusions and Future Prospects

We studied the problem of dragging an ideal polymer, both in free space and in a vicinity of a wall, and found the critical pulling velocities for which we can reconstruct the correct $\Delta F$ using Jarzynski equality. We saw that the critical velocity is related to the exponent $\nu$ via $v_c \sim N^{-\frac{1}{2}}$ for ND case and $v_c \sim N^{-\nu-1}$ for OLD. This result is valid in free space as well as near the wall. Gaussian polymers could be solved analytically in the free space but near the wall it becomes an unsolvable problem. We believe that the same qualitative arguments that lead us to the critical velocities near the wall, are also valid for the case of SAW polymers. Therefore, the assumption is that the critical velocities behavior is the same with the appropriate exponent $\nu$. This could be an interesting research direction since SAW polymer model describes a more realistic behavior of polymers.

Notice, that we never mentioned the dependence of the critical velocities on the sample size. We were interested only in the limits of $v > v_c$ for which we cannot practically calculate $\Delta F$, and $v \ll v_c$ when we can reconstruct $\Delta F$ correctly. The reason for that is that around $v_c$ the sample size depends exponentialy on the dissipative work, as shown by Yunger Halpern and Jarzynski [49]. Thus, the sample size changes very fast around $v_c$, but far from $v_c$ it does not play an important role in reconstruction of $\Delta F$.

The probability distribution of work seems to be independent of $N$ for fixed $u$ and $\ell$. We believe that there is an asymptotic behavior of $P(W_{\mathrm{d}})$ when $N \gg 1$. Still, we cannot determine that this behavior exists because we studied polymers up to $N = 100$ monomers. It can be very interesting to see what happens with longer polymers.

# Appendix A

# Dimensionless Variables

## A.1 Newtonian dynamics

Consider a harmonic oscillator with mass $m$ and spring constant $k$ at temperature $T$. The natural frequency of the oscillator is $\omega = \sqrt{k/m}$. Using these basic quantities, we define dimensionless variables as detailed in table A.1.

**Table A.1:** The conversion rules from the dimensionless variables to dimensional variables, for the case of simple harmonic oscillator.

| Quantity | Dimensionless | With Dimensions |
|---|---|---|
| Length | $x$ | $\omega^{-1}\sqrt{k_{\mathrm{B}}T/m}x$ |
| Time | $t$ | $\omega^{-1}t$ |
| Velocity | $v$ | $\sqrt{k_{\mathrm{B}}T/m}v$ |
| Energy | $E$ | $k_{\mathrm{B}}TE$ |
| Force | $f$ | $\omega\sqrt{mk_{\mathrm{B}}T}f$ |

## A.2 Overdamped Langevin dynamics

In the overdamped case, we add the friction coefficient $\gamma$ and we define the relaxation time $\tau = \gamma/k$. Using these basic quantities, we define dimensionless variables as detailed in table A.2.

**Table A.2:** The conversion rules from the dimensionless variables to dimensional variables, for the case of overdamped harmonic oscillator.

| Quantity | Dimensionless | With Dimensions |
|---|---|---|
| Length | $x$ | $\sqrt{k_{\mathrm{B}}T/k}x$ |
| Time | $t$ | $\tau t$ |
| Velocity | $v$ | $\sqrt{\tau^{-1}\gamma^{-1}k_{\mathrm{B}}T}v$ |
| Energy | $E$ | $k_{\mathrm{B}}TE$ |
| Force | $f$ | $\sqrt{\tau^{-1}\gamma k_{\mathrm{B}}T}f$ |

# Appendix B

# Decomposing to Normal Modes

Consider a 1D Gaussian chain with $N$ identical monomers. The positions of the monomers in the laboratory reference frame are $\{x_n\}_{n=1}^{N}$. We define two additional "ghost" monomers: one is the zeroth monomer which its position is given by $x_0 = vt$, and the other one is the $(N+1)$th monomer $x_{N+1} = x_N$, that ensures the "free end" condition, i.e., there is only force acting on the $N$th monomer from the $(N-1)$th monomer. This way, equations (3.10) and (3.46) including also the $N$th monomer.

We denote by $\tilde{x}_n = x_n - vt$ the position of the $n$th monomer with respect to a *moving reference frame* that moves with the zeroth monomer, i.e., with a constant velocity $v$. Working in the moving reference frame, we can perform a discrete sine Fourier transform that fulfills the boundary conditions ($\tilde{x}_0 = 0$ and $\tilde{x}_{N+1} = \tilde{x}_N$)

$$\tilde{x}_n = A \sum_{q=1}^{N} \tilde{x}_q \sin\left(\alpha_q n\right), \tag{B.1}$$

where

$$A = \sqrt{\frac{2}{N+\frac{1}{2}}} \quad ; \quad \alpha_q = \frac{\pi(q-\frac{1}{2})}{N+\frac{1}{2}} \ . \tag{B.2}$$

The values of $\alpha_q$ were chosen this way to satisfy the boundry conditions. The same decomposion can be done for the pulling velocity

$$v = A \sum_{q=1}^{N} v_q \sin\left(\alpha_q n\right), \tag{B.3}$$

where

$$v_q = \frac{1}{2} A v \cot\left(\frac{\alpha_q}{2}\right). \tag{B.4}$$

Notice, that (B.3) valid only for $1 \leq n \leq N$. Using the connection between $x_n$ and

$\tilde{x}_n$, we can find the relation between $x_q$ and $\tilde{x}_q$:

$$\begin{aligned} x_n &= \tilde{x}_n + vt && \text{(B.5)} \\ &= A\sum_{q=1}^{N} \tilde{x}_q \sin(\alpha_q n) + A\sum_{q=1}^{N} v_q \sin(\alpha_q n)\, t && \text{(B.6)} \\ &= A\sum_{q=1}^{N} \underbrace{(\tilde{x}_q + v_q t)}_{x_q} \sin(\alpha_q n)\,. && \text{(B.7)} \end{aligned}$$

Thus, we get

$$x_q = \tilde{x}_q + v_q t. \tag{B.8}$$

## B.1 Newtonian dynamics

For the Newtonian dynamics case (as depicted in sub-section 3.1.2), the equations of motion in the moving reference frame are

$$\ddot{\tilde{x}}_n = -2\tilde{x}_n + \tilde{x}_{n+1} + \tilde{x}_{n-1}. \tag{B.9}$$

Substituting (B.1) into (B.9) yields

$$\sum_{q=1}^{N} \left[\ddot{\tilde{x}}_q + 4\sin^2\left(\frac{\alpha_q}{2}\right)\tilde{x}_q\right]\sin(\alpha_q n) = 0. \tag{B.10}$$

Since the eigenmodes are orthogonal, every coefficient in the sum above must vanish, and therefore

$$\ddot{\tilde{x}}_q = -4\sin^2\left(\frac{\alpha_q}{2}\right)\tilde{x}_q \equiv -\omega_q^2 \tilde{x}_q, \tag{B.11}$$

where the frequency $\omega_q$ is given by

$$\omega_q^2 = 4\sin^2\left(\frac{\pi(q-\frac{1}{2})}{2(N+\frac{1}{2})}\right). \tag{B.12}$$

The solution for the amplitudes $x_q$ in the laboratory reference frame is

$$x_q(t) = x_q^0 \cos(\omega_q t) + \frac{1}{\omega_q}\left(p_q^0 - v_q\right)\sin(\omega_q t) + v_q t, \tag{B.13}$$

where $x_q^0 = x_q(t=0)$ and $p_q^0 = \dot{x}_q^0 = p_q(t=0)$. The total work done on the polymer in the laboratory reference frame can be split into sum of works performed on each eigenmode

$$W(t) = -v\int_0^t (x_1 - vt')\,dt' = -\sum_{q=1}^{N} v\sin(\alpha_q)\int_0^t (x_q - v_q t')\,dt' \equiv \sum_{q=1}^{N} W_q. \quad \text{(B.14)}$$

For each eigenmode

$$\begin{aligned} W_q(t) &= -vA\sin(\alpha_q)\int_0^t \tilde{x}_q dt' \\ &= -2vA\sin\left(\frac{\alpha_q}{2}\right)\cos\left(\frac{\alpha_q}{2}\right)\int_0^t \tilde{x}_q dt' \\ &= -4\sin^2\left(\frac{\alpha_q}{2}\right)\frac{1}{2}vA\cot\left(\frac{\alpha_q}{2}\right)\int_0^t \tilde{x}_q dt' \\ &= -\omega_q^2 v_q \int_0^t \tilde{x}_q dt'. \end{aligned} \quad \text{(B.15)}$$

Using (B.13) we get

$$W_q(x_q^0, p_q^0) = -v_q\left[\omega_q x_q^0 \sin(\omega_q t') - (p_q^0 - v_q)\cos(\omega_q t')\right]. \quad \text{(B.16)}$$

The probability distribution of values $W$ of $W_q$ st time $t$ is given by

$$P_q(W) = \left\langle \delta\left(W - W_q\left(x_q^0, p_q^0\right)\right)\right\rangle, \quad \text{(B.17)}$$

where the averaging of the $\delta$-function is performed with respect to the initial Boltzmann distribution of $\left\{x_q^0\right\}_{q=1}^N$ and $\left\{p_q^0\right\}_{q=1}^N$. Using the presentation of the $\delta$-function via Fourier theorem $\delta(y) = \frac{1}{2\pi}\int_{-\infty}^{\infty} e^{iky}dk$, we get

$$P_q(W) = \frac{1}{2\pi}\int_{-\infty}^{\infty} e^{ikW}\left\langle e^{-ikW_q(x_q^0, p_q^0)}\right\rangle dk. \quad \text{(B.18)}$$

Substituting $W_q(x_q^0, p_q^0)$ into (B.18)

$$\begin{aligned}\left\langle e^{-ikW_q(x_q^0,p_q^0)}\right\rangle &= \frac{\omega_q}{2\pi}e^{ikv_q^2[\cos(\omega_q t)-1]}\int_{-\infty}^{\infty}e^{\frac{-\omega_q^2(x_q^0)^2}{2}+ix_q^0k\omega_q v_q\sin(\omega_q t)}dx_q^0 \\ &\times \int_{-\infty}^{\infty}e^{\frac{-(p_q^0)^2}{2}+ip_{0q}kv[\cos(\omega_q t)-1]}dp_q^0 \\ &= \exp\left\{v_q^2[\cos(\omega_q t)-1](k^2+ik)\right\}. \end{aligned} \tag{B.19}$$

Now we can calculate

$$\begin{aligned}P_q(W) &= \frac{1}{2\pi}\int_{-\infty}^{\infty}e^{ikW}e^{\left[v_q^2(\cos(\omega_q t)-1)(k^2+ik)\right]}dk \\ &= \frac{1}{\sqrt{2\pi}\sigma_q}\exp\left[-\frac{(W-\mu_q)^2}{2\sigma_q^2}\right], \end{aligned} \tag{B.20}$$

where

$$\mu_q = \frac{1}{2}\sigma_q^2 \equiv 2v_q^2\sin^2\left(\frac{\omega_q t}{2}\right). \tag{B.21}$$

Now we would like to find the total work distribution $P\left(W=\sum_{q=1}^{N}W_q\right)$ for $N$ oscillators, which is given by the convolution

$$P\left(W=\sum_{q=1}^{N}W_q\right) = P_1(W_1) * P_2(W_2) * \cdots * P_N(W_N). \tag{B.22}$$

Applying Fourier transform on the convolution (B.22) yields a multiplication in Fourier space

$$\tilde{P}(k) = \prod_{q=1}^{N}\tilde{P}_q(k), \tag{B.23}$$

where

$$\tilde{P}_q(k) = \int_{-\infty}^{\infty}P_q(W)e^{-ikW}dW = \exp\left(-\frac{k^2\sigma_q^2}{2}-ik\mu_q\right). \tag{B.24}$$

Thus, the total distribution in Fourier space is

$$\tilde{P}(k) = \prod_{q=1}^{N}\exp\left(-\frac{k^2\sigma_q^2}{2}-ik\mu_q\right) = \exp\left(-\frac{k^2}{2}\sum_{q=1}^{N}\sigma_q^2 - ik\sum_{q=1}^{N}\mu_q\right). \tag{B.25}$$

Let us denote

$$\mu(t) \equiv \sum_{q=1}^{N} \mu_q(t), \tag{B.26}$$

and

$$\sigma^2(t) \equiv \sum_{q=1}^{N} \sigma_q^2(t) = 2\sum_{q=1}^{N} \mu_q(t) = 2\mu(t). \tag{B.27}$$

In this notation, we can simply recognize (B.25) as a Fourier transform of a Gaussian, an therefore

$$P(W) = \frac{1}{\sqrt{2\pi}\sigma} \exp\left(-\frac{(W-\mu)^2}{2\sigma^2}\right). \tag{B.28}$$

Notice, that $\mu = \frac{1}{2}\sigma^2$, as is expected for the case where $\Delta F = 0$ (2.14).

## B.2 Overdamped Langevin dynamics

The same decomposition can be done to Gaussian chain which its dynamics is depicted by the overdamped Langevin equation. In this case the eigenmodes called *Rouse modes* [6]. The equation of motion of the $n$th monomer in the moving reference frame is

$$\dot{\tilde{x}}_n = -2\tilde{x}_n + \tilde{x}_{n+1} + \tilde{x}_{n-1} + R_n(t) - v, \tag{B.29}$$

where again, we added two "ghost" monomers, ($\tilde{x}_0 = 0$ and $\tilde{x}_{N+1} = \tilde{x}_N$), and $R_n(t)$ is the random force that acting on the $n$'th particle, which satisfies

$$\langle R_n(t)\rangle = 0 \quad ; \quad \langle R_n(t)R_m(t')\rangle = 2\delta_{n,m}\delta(t-t') \ . \tag{B.30}$$

The random noise can also be decomposed using discrete sine Fourier transform

$$R_n = A\sum_{q=1}^{N} r_q \sin(\alpha_q n), \tag{B.31}$$

where $\alpha_q$ and $A$ are given by (B.2), $r_q$ is the amplitude of the $q$th mode of the noise, and the noise correlation in Fourier space is given by

$$\big\langle r_q(t)\big\rangle = 0 \quad ; \quad \big\langle r_q(t)r_l(t')\big\rangle = 2\delta_{q,l}\delta(t-t') \ . \tag{B.32}$$

Substituting (B.1) into (B.29) yields equations for the amplitudes

$$\sum_{q=1}^{N}\left[\dot{\tilde{x}}_q + 4\sin^2\left(\frac{\alpha_q}{2}\right)\tilde{x}_q - r_q + v_q\right]\sin\left(a_q n\right) = 0, \tag{B.33}$$

where $v_q$ is given by (B.4). Using the orthogonality of the eigenmodes, we get a set of $N$ independent equations

$$\dot{\tilde{x}}_q + 4\sin^2\left(\frac{\alpha_q}{2}\right)\tilde{x}_q - r_q + v_q = 0, \tag{B.34}$$

for $q = 1, 2, ..., N$. We define the inverse relaxation time of the $q$th mode

$$\frac{1}{\tau_q} \equiv 4\sin^2\left(\frac{\alpha_q}{2}\right). \tag{B.35}$$

Recall that the elementary relaxation time of a single oscillator is 1. With (B.35), the Lagevin equation for each $\tilde{x}_q$ simplifies to

$$\dot{\tilde{x}}_q = -\frac{1}{\tau_q}\tilde{x}_q + r_q - v_q. \tag{B.36}$$

The solution of this equation is

$$\tilde{x}_q(t) = \tilde{x}_q^0 e^{-\frac{t}{\tau_q}} + \frac{1}{\tau_q}e^{-\frac{t}{\tau_q}}\int_0^t \big(r_q(t') - v_q\big)e^{\frac{t'}{\tau_q}}dt', \tag{B.37}$$

where $\tilde{x}_q^0 = \tilde{x}_q(t=0)$.

# Appendix C
# Numerical Methods

## C.1 Runge-Kutta method

In this thesis we solve either second-order differential equations (Newtonian dynamics case), or first-order differential equations (overdamped Langevin dynamics case). These differential equations can be solved numerically by time discretization. There are many numerical methods to solve such difference equations, one of them is the Runge-Kutta method [50]. The Runge-Kutta algorithm has different orders of accuracy. We will use 4th order Runge-Kutta method, which requires calculation of 4 different approximations to the derivative at each time-step.

Suppose we have the following first-order differential equation

$$\frac{\mathrm{d}x(t)}{\mathrm{d}t} = f(x,t), \tag{C.1}$$

with some initial condition $x(t_0) = x_0$. Now we want to find $x(t_0+\Delta t)$. The first order approximation (Euler method) is telling us multiply the slope at $t = t_0$ by the step size $\Delta t$ and add it to the initial position $x(t_0)$ so that $x(t_0+\Delta t) = x_0 + f(x_0,t_0)\cdot\Delta t$. This is actually the first order of Taylor expansion. To be more accurate we use the 4th order Runge-Kutta method which takes a weighted mean of four different slopes:

$$\begin{aligned}
k_1 &= f\left(x(t_0), t_0\right), && \text{(C.2)}\\
k_2 &= f\left(x(t_0) + k_1\frac{\Delta t}{2}, t_0 + \frac{\Delta t}{2}\right), && \text{(C.3)}\\
k_3 &= f\left(x(t_0) + k_2\frac{\Delta t}{2}, t_0 + \frac{\Delta t}{2}\right), && \text{(C.4)}\\
k_4 &= f\left(x(t_0) + k_3\Delta t, t_0 + \Delta t\right), && \text{(C.5)}
\end{aligned}$$

where

- $k_1$ is the slope at the beginning of the time step.
- $k_2$ is the slope at the midpoint $t = t_0 + \frac{\Delta t}{2}$ using $k_1$.
- $k_3$ is the slope at the midpoint $t = t_0 + \frac{\Delta t}{2}$ using $k_2$.

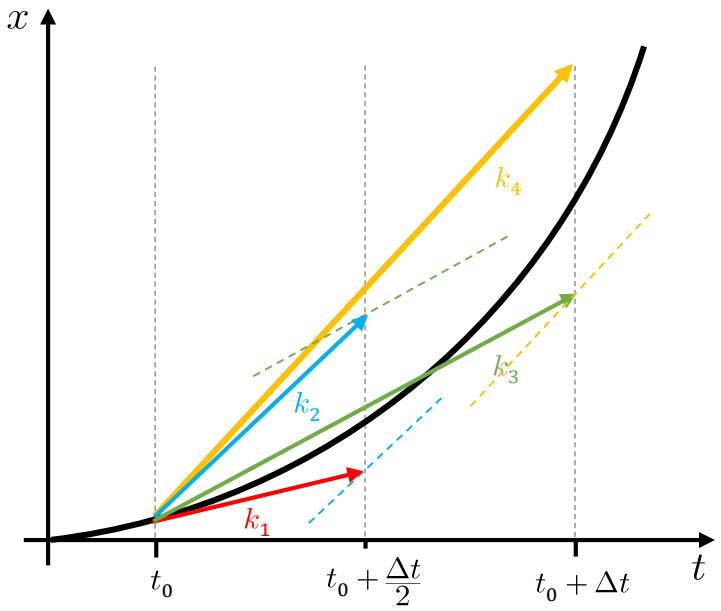


**Figure C.1:** Demonstration of Runge-Kutta 4th order method. We use the the incline $k_1$ at the initial point $t_0$ to make the red step to $t_0 + \Delta t/2$, then we calculate the incline $k_2$ at the midpoint and use it again to make a step (blue) from the initial point to $t_0 + \Delta t/2$, calculating the incline $k_3$ there. Finally, we use $k_3$ to make a big step (green) $\Delta t$ and calculate the incline at $t_0 + \Delta t$ which gives us $k_4$.

- $k_4$ is the slope at the endpoint $t = t_0 + \Delta t$ using $k_3$.

The total slope will be a weighted mean $\bar{k} = \frac{1}{6}(k_1 + 2k_2 + 2k_3 + k_4)$. In other words, we take an underestimated and overestimated slopes ($k_1$ and $k_4$) and another pair of slopes in the middle ($k_2$ and $k_3$). The total step will be

$$x(t_0 + \Delta t) = x_0 + \frac{1}{6}(k_1 + 2k_2 + 2k_3 + k_4)\,\Delta t + \mathcal{O}(\Delta t^5). \tag{C.6}$$

For a second-order ordinary differential equation, such as

$$\frac{\mathrm{d}^2 x(t)}{\mathrm{d}t^2} = a(x,t), \tag{C.7}$$

we can reduce the order of the equation by denoting $\frac{\mathrm{d}x(t)}{\mathrm{d}t} = v(x,t)$, and solve two first-order differential equations.

## C.2 Treatment of noise in Langevin equation near a wall

In this section we would like to explain the way we choose the thermal noise in a numerical simulation, which solves the overdamped Langevin equation near a wall. The overdamped Langevin equation is a first-order differential equation, which is generally given by

$$\frac{\mathrm{d}x}{\mathrm{d}t} = -\frac{\mathrm{d}V(x,t)}{\mathrm{d}x} + R(t), \tag{C.8}$$

where $V(x,t)$ is some general potential and $R(t)$ is a thermal noise, which satisfies

$$\langle R(t)\rangle = 0 \quad ; \quad \langle R(t)R(t')\rangle = 2\delta(t-t') \ . \tag{C.9}$$

To demonstrate the treatment of noise, we will use the simplest method to solve such first-order differential equation, i.e., the Euler method [50]. If we choose the time-step size to be $\Delta t$, we get the following difference equation

$$x(t+\Delta t) = x(t) - \frac{\mathrm{d}V(x,t)}{\mathrm{d}x}\Delta t + R(t)\Delta t + \mathcal{O}(\Delta t^2), \tag{C.10}$$

Usually, when we use time discretization to solve such differential equation, at each iteration the thermal noise $R(t)$ is chosen from a Gaussian distribution with mean $\langle R(t)\rangle = 0$ and variance $\langle R^2(t)\rangle = 2/\Delta t$. A problem arises, when we want to choose the noise near a wall. For small enough $\Delta t$, the change in the position over one iteration is dominated by the thermal noise, i.e., $\Delta x \approx R(t)\Delta t$. The value of $\Delta x$ is also chosen from a Gaussian distribution with variance $\langle \Delta x^2\rangle = 2\Delta t$. In the vicinity of the wall, there is a probability that the next step will bring the particle to the forbidden side of the wall, i.e., if the wall is located at $x = 0$, then $x(t+\Delta t) < 0$. The term $\Delta x \approx R(t)\Delta t$ is actually depicts a diffusion. In order to determine the position of the particle after it collides with the wall, we demand that the current of the particle into the wall vanishes. This can be done by using the method of images. Practically, if the particle moves a step $\Delta x$ that brings it to the other side of the wall, we simply move it to the other side by $|x(t) + \Delta x|$ (as depicted in Figure C.2). In other words, we take the absolute value of $x(t+\Delta t)$.

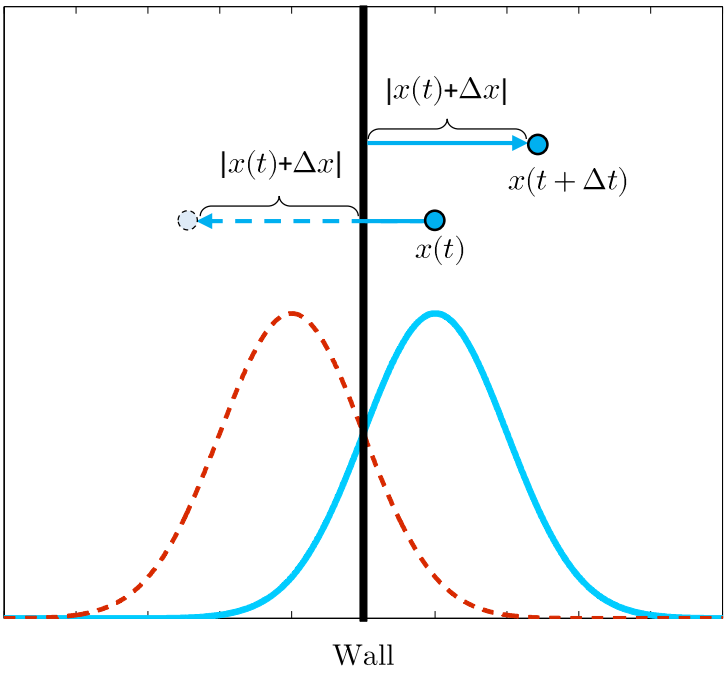


**Figure C.2:** A particle at $x(t)$ making a finite step $\Delta x$ which brings to the other side of the wall, which is located at $x = 0$. The new position $x(t + \Delta t) = x(t) + \Delta x$. The dashed red curve represents the image particle, which ensure that there is no current on the wall.

# Appendix D

# Partition Function near a Wall

The partition function of an ideal polymer in free space in dimensionless units is

$$
\begin{aligned}
Z_{\text{free}} &\propto \int_{-\infty}^{\infty} e^{-\sum_{i=1}^{N} \frac{p_i^2}{2}} \prod_{i=1}^{N} \mathrm{d}p_i \int_{-\infty}^{\infty} e^{-\sum_{i=1}^{N} \frac{(x_i - x_{i-1})^2}{2}} \prod_{i=1}^{N} \mathrm{d}x_i && \text{(D.1)} \\
&= \Big( \int_{-\infty}^{\infty} e^{-\frac{p^2}{2}} \mathrm{d}p \Big)^N \Big( \int_{-\infty}^{\infty} e^{-\frac{x^2}{2}} \mathrm{d}x \Big)^N && \text{(D.2)} \\
&= (2\pi)^N. && \text{(D.3)}
\end{aligned}
$$

The partition function near the wall

$$
\begin{aligned}
Z_{\text{wall}} &\propto \int_{-\infty}^{\infty} e^{-\sum_{i=1}^{N} \frac{p_i^2}{2}} \prod_{i=1}^{N} \mathrm{d}p_i \int_{0}^{\infty} e^{-\sum_{i=1}^{N} \frac{(x_i - x_{i-1})^2}{2}} \prod_{i=1}^{N} \mathrm{d}x_i && \text{(D.4)} \\
&= \Big( \int_{-\infty}^{\infty} e^{-\frac{p^2}{2}} \mathrm{d}p \Big)^N I(N) && \text{(D.5)} \\
&= (2\pi)^{N/2} I(N), && \text{(D.6)}
\end{aligned}
$$

where $I(N)$ is given by

$$
I(N) = \int_0^{\infty} e^{-\frac{(x_1 - x_0)^2}{2}} \int_0^{\infty} e^{-\frac{(x_2 - x_1)^2}{2}} \cdots \int_0^{\infty} e^{-\frac{(x_N - x_{N-1})^2}{2}} \prod_{i=1}^{N} \mathrm{d}x_i. \tag{D.7}
$$

The wall can be modeled as a potential $V_{\text{wall}}(x_i)$ defined as,

$$
V_{\text{wall}}(x_i) = \begin{cases} 0, & \text{if } \{x_i\} > 0 \ , \\ \infty, & \text{if at least one } x_i \leq 0 \ . \end{cases} \tag{D.8}
$$

The total Hamiltonian of the system is

$$
\mathcal{H} = \mathcal{H}_0 + V_{\text{wall}}, \tag{D.9}
$$

where $\mathcal{H}_0$ is the Hamiltonian of a Gaussian chain in free space. The partition functions near the wall can be written as

$$\begin{aligned} Z_{\text{wall}} &= \text{Tr}e^{-(\mathcal{H}_0+V_{\text{wall}})} && \text{(D.10)} \\ &= Z_{\text{free}}\frac{1}{Z_{\text{free}}}\text{Tr}e^{-\mathcal{H}_0}e^{-V_{\text{wall}}} && \text{(D.11)} \\ &= Z_{\text{free}}\left\langle e^{-V_{\text{wall}}}\right\rangle_0, && \text{(D.12)} \end{aligned}$$

where $\langle\cdots\rangle_0$ denotes a thermal average with respect to $\mathcal{H}_0$, $Z_{\text{free}} = \text{Tr}e^{-\mathcal{H}_0}$ is the partition function in free space, and

$$e^{-V_{\text{wall}}(x_i)} = \begin{cases} 1, & \text{if } \{x_i\} > 0, \\ 0, & \text{if at least one } x_i \leq 0. \end{cases} \tag{D.13}$$

In order to calculate $\left\langle e^{-V_{\text{wall}}}\right\rangle_0$ numerically, we generated $n$ samples of a polymer in free space, and count only $m$ samples where all the $x_i$s are positive. The average $\left\langle e^{-V_{\text{wall}}}\right\rangle_0 = m/n$. Thus, the free energy difference is given by

$$\Delta F = -\ln\left(\frac{Z_{\text{free}}}{Z_{\text{wall}}}\right) = \ln\left(\left\langle e^{-V_{\text{wall}}}\right\rangle_0\right) = \ln\left(\frac{m}{n}\right). \tag{D.14}$$

Our numerical results are depicted in Figure D.1, on semi-logarithmic scale. We know that for large $N$ the free energy difference is $\Delta F = -0.5\ln N + \mathcal{C}$. We compare our numerical evaluations of $\Delta F$ with the theoretical curve, and by fitting the results, find $\mathcal{C} \approx -0.589$.

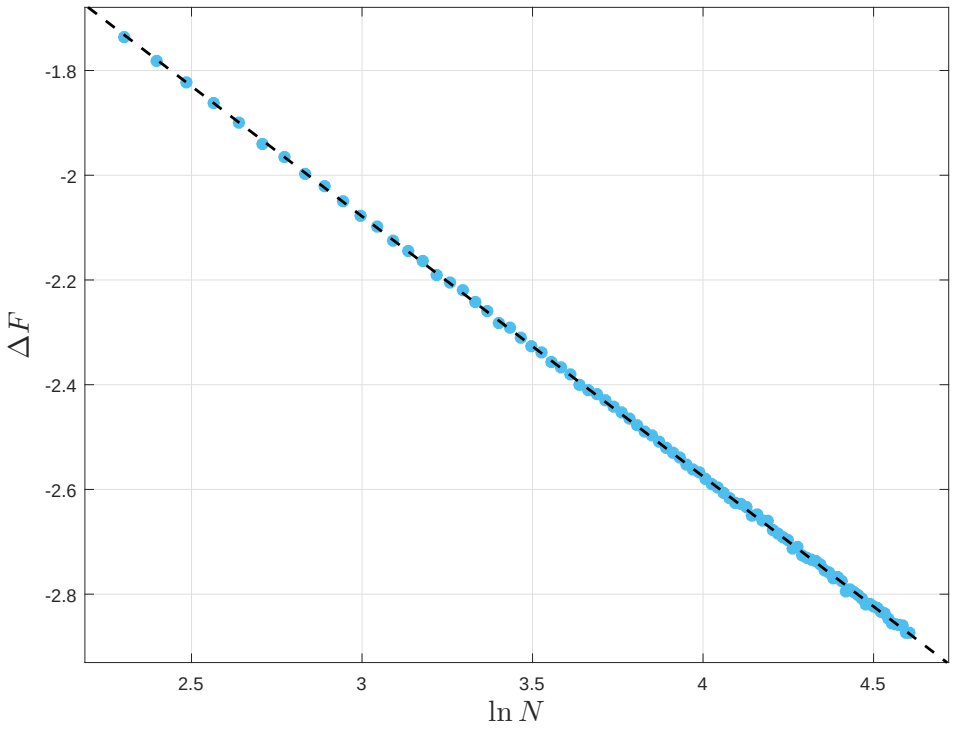


**Figure D.1:** The free energy difference $\Delta F$ versus logarithm of the number of monomers $N$. The blue dots depicts the numerical data, while the dashed line depict the fit function $\Delta F = -0.499 \ln N - 0.589$.

# Bibliography


[1] J. Liphardt, S. Dumont, S. B. Smith, I. Tinoco Jr., and C. Bustamante, "Equilibrium information from nonequilibrium measurements in an experimental test of Jarzynski's equality," *Science*, vol. 296, pp. 1832–1835, 2002.

[2] C. Jarzynski, "Nonequilibrium equality for free energy differences," *Phys. Rev. Lett.*, vol. 78, pp. 2690–2693, 1997.

[3] C. Jarzynski, "Equilibrium free-energy differences from nonequilibrium measurements: A master-equation approach," *Phys. Rev. E*, vol. 56, pp. 5018–5035, 1997.

[4] P. G. de Gennes, *Scaling concepts in polymer physics*. New York: Cornell University Press, 1979.

[5] M. Rubinstein and R. H. Colby, *Polymer physics*. New York: Oxford University Press, 2003.

[6] M. Doi and S. Edwards, *The theory of polymer dynamics*. Oxford: Oxford University Press, 1986.

[7] F. Spitzer, *Principles of random walk*. New York: Springer Verlag, 2011.

[8] B. Hughes, *Random walks and random environments*. New York: Oxford University Press, 1995.

[9] M. Doi, *Introduction to polymer physics*. Oxford: Oxford University Press, 1996.

[10] J. Zlatanova and K. van Holde, "Single-molecule biology: what is it and how does it work?," *Mol. Cell*, vol. 24, pp. 317–329, 2006.

[11] G. Binnig, C. F. Quate, and C. Gerber, "Atomic force microscope," *Phys. Rev. Lett.*, vol. 56, p. 930, 1986.

[12] C. Bustamante, S. B. Smith, J. Liphardt, and D. Smith, "Single molecule studies of DNA mechanics," *Curr. Opin. Struc. Biol.*, vol. 10, pp. 279–285, 2000.

[13] M. F. Maghrebi, Y. Kantor, and M. Kardar, "Entropic force of polymers on a cone tip," *Europhys. Lett.*, vol. 96, p. 66002, 2011.

[14] M. F. Maghrebi, Y. Kantor, and M. Kardar, "Polymer-mediated entropic forces between scale-free objects," *Phys. Rev. E*, vol. 86, pp. 1–13, 2012.

[15] Y. Hammer and Y. Kantor, "Ideal polymers near scale-free surfaces," *Phys. Rev. E*, vol. 89, p. 022601, 2014.

[16] S. Chandrasekhar, "Stochastic problems in physics and astronomy," *Rev. Mod. Phys.*, vol. 15, pp. 1–89, 1943.

[17] C. Jarzynski, "Nonequilibrium work relations: foundations and applications," *Eur. Phys. J. B*, vol. 64, pp. 331–340, 2008.

[18] G. Hummer, "Fast-growth thermodynamic integration: Error and efficiency analysis," *Chem. Phys.*, vol. 114, pp. 7330–7337, 2001.

[19] J. Hermans, "Simple analysis of noise and hysteresis in (slow-growth) free energy simulations," *J. Phys. Chem.*, vol. 95, pp. 9029–9032, 1991.

[20] R. H. Wood, W. C. F. Mühlbauer, and P. T. Thompson, "Systematic errors in free energy perturbation calculations due to a finite sample of configuration space: Sample-size hysteresis," *J. Phys. Chem.*, vol. 95, pp. 6670–6675, 1991.

[21] G. Hummer and A. Szabo, "Free energy reconstruction from nonequilibrium single-molecule pulling experiments," *PNAS*, vol. 98, pp. 3658–3661, 2001.

[22] G. Hummer and A. Szabo, "Free energy surfaces from single-molecule force spectroscopy," *Acc. Chem. Res.*, vol. 38, pp. 504–513, 2005.

[23] G. Hummer and A. Szabo, "Free energy reconstruction from nonequilibrium single-molecule pulling experiments," *PNAS*, vol. 98, pp. 3658–3661, 2005.

[24] F. Douarche, S. Ciliberto, and A. Petrosyan, "Estimate of the free energy difference in mechanical systems from work fluctuations: experiments and models," *J. Stat. Mech.: Theor. Exp.*, p. P09011, 2005.

[25] F. Douarche, S. Ciliberto, A. Petrosyan, and I. Rabbiosi, "An experimental test of the Jarzynski equality in a mechanical experiment," *Europhys. Lett.*, vol. 70, pp. 593–599, 2005.

[26] C. Bustamante, J. Liphardt, and F. Ritort, "The nonequilibrium thermodynamics of small systems," *Physics Today*, vol. 58, p. 43, 2005.

[27] V. Blickle, T. Speck, L. Helden, U. Seifert, and C. Bechinger, "Thermodynamics of a colloidal particle in a time-dependent nonharmonic potential," *Phys. Rev. Lett.*, vol. 96, p. 70603, 2006.

[28] N. C. Harris, Y. Song, and C.-H. Kiang, "Experimental free energy surface reconstruction from single-molecule force spectroscopy using Jarzynski's equality," *Phys. Rev. Lett.*, vol. 99, p. 68101, 2007.

[29] O. P. Saira, Y. Yoon, T. Tanttu, M. Möttönen, D. V. Averin, and J. P. Pekola, "Test of the Jarzynski and Crooks fluctuation relations in an electronic system," *Phys. Rev. Lett.*, vol. 109, p. 180601, 2012.

[30] I. Bena, C. van den Broeck, and R. Kawai, "Jarzynski equality for the Jepsen gas," *Europhys. Lett.*, vol. 71, pp. 879–885, 2005.

[31] D. A. Hendrix and C. Jarzynski, "A 'fast growth' method of computing free energy differences," *J. Chem. Phys.*, vol. 114, pp. 5974–5981, 2001.

[32] D. Jeong and I. Andricioaei, "Reconstructing equilibrium entropy and enthalpy profiles from non-equilibrium pulling," *J. Chem. Phys.*, vol. 138, p. 114110, 2013.

[33] G. Xiao and J. Gong, "Suppression of work fuctuations by optimal control: An approach based on Jarzynski's equality," *Phys. Rev. E*, vol. 90, p. 52132, 2014.

[34] R. C. Lua and A. Y. Grosberg, "Practical applicability of the Jarzynski relation in statistical mechanics: A pedagogical example," *J. Chem. Phys. B*, vol. 109, pp. 6805–6811, 2004.

[35] S. An, J.-N. Zhang, M. Um, D. Lv, Y. Lu, J. Zhang, Z.-q. Yin, H. T. Quan, and K. Kim, "Experimental test of quantum Jarzynski equality with a trapped ion system," *Nat. Phys.*, vol. 11, p. 193, 2015.

[36] D. Cohen and Y. Imry, "Straightforward quantum-mechanical derivation of the Crooks fluctuation theorem and the Jarzynski equality," *Phys. Rev. E*, vol. 86, p. 11111, 2012.

[37] T. Speck and U. Seifert, "Dissipated work in driven harmonic diffusive systems: General solution and application to stretching Rouse polymers," *Eur. J. Phys. B*, vol. 43, pp. 521–527, 2005.

[38] A. Dhar, "Work distribution functions in polymer stretching experiments," *Phys. Rev. E*, vol. 71, p. 36126, 2005.

[39] B. Saha and S. Mukherji, "Work distribution function for a Brownian particle driven by a nonconservative force," *Eur. Phys. J. B*, vol. 88, p. 146, 2015.

[40] S. Kim, Y. W. Kim, P. Talkner, and J. Yi, "Comparison of free-energy estimators and their dependence on dissipated work," *Phys. Rev. E*, vol. 86, p. 41130, 2012.

[41] O. Mazonka and C. Jarzynski, "Exactly solvable model illustrating far-from-equilibrium predictions," *ArXiv*, p. condmat/991212, 1999.

[42] R. van Zon and E. G. D. Cohen, "Stationary and transient work-fluctuation theorems for a dragged Brownian particle," *Phys. Rev. E*, vol. 67, p. 46102, 2003.

[43] G. M. Wang, E. M. Sevick, E. Mittag, D. J. Searles, and D. J. Evans, "Experimental demonstration of violations of the second law of thermodynamics for small systems and short time scales," *Phys. Rev. Lett.*, vol. 89, p. 50601, 2002.

[44] B. Saha and S. Mukherji, "Work and heat distributions for a Brownian particle subjected to an oscillatory drive," *J. Stat. Mech.: Theor. Exp.*, p. P08014, 2014.

[45] S. Sabhapandit, "Work fluctuations for a harmonic oscillator driven by an external random force," *Europhys. Lett.*, vol. 96, p. 20005, 2011.

[46] A. Imparato and L. Peliti, "Fluctuation relations for a driven Brownian particle," *Phys. Rev. E*, vol. 74, p. 26106, 2006.

[47] A. Imparato, L. Peliti, G. Pesce G. Rusciano, and A. Sasso, "Work and heat probability distribution of an optically driven Brownian particle: Theory and experiments," *Phys. Rev. E*, vol. 76, p. 50101, 2007.

[48] H. Goldstein, C. Poole, and J. Safko, *Classical mechanics*. New York: Addison Wesley, 2007.

[49] N. Yunger Halpern and C. Jarzynski, "Number of trials required to estimate a free-energy difference, using fluctuation relations," *Phys. Rev. E*, vol. 93, p. 52144, 2016.

[50] W. H. Press, S. A. Teukolsky, W. T. Vetterling, and B. P. Flannery, *Numerical recipes in C*. New York: Cambridge University Press, 1992.